Metamodèle de la propagation d'ondes sismiques 3D par opérateur neuronal de Fourier (FNO) amélioré avec un transfert d'apprentissage

Filippo Gatti[†] [1], Fanny Lehmann[†,‡], M. Bertin[‡], D. Clouteau[†]

[†]Laboratoire de Mécanique Paris-Saclay UMR 9026
Université Paris-Saclay, CentraleSupélec, ENS Paris-Saclay, CNRS
[‡] CEA/DAM/DIF

June 26, 2024

1. filippo.gatti@centralesupelec.fr

Outline

1. General context
2. Earthquake neural simulator
3. What's next ?
4. Annexes
5. Bibliography

General context

Earthquake risk

M_W7.8-7.7 Türkiye-Syria earthquake (February 2023)

- World Bank estimated $34+ bn losses (4% of Turkey's total GDP)
- Catastrophe modeller RMS estimated $25 bn losses
- Insured losses projected to exceed $5 bn
  - Residential building : $18+bn
  - Non residential buildings : $9.7 bn
  - Infrastructures : $6.4 bn
- Public compulsory earthquake insurance (paying capacity : $2.5 bn)



Source : reinsurancene.ws

SEM3D [4, 10] : an open-source HPC code for earthquake simulation (https://github.com/sem3d/SEM)

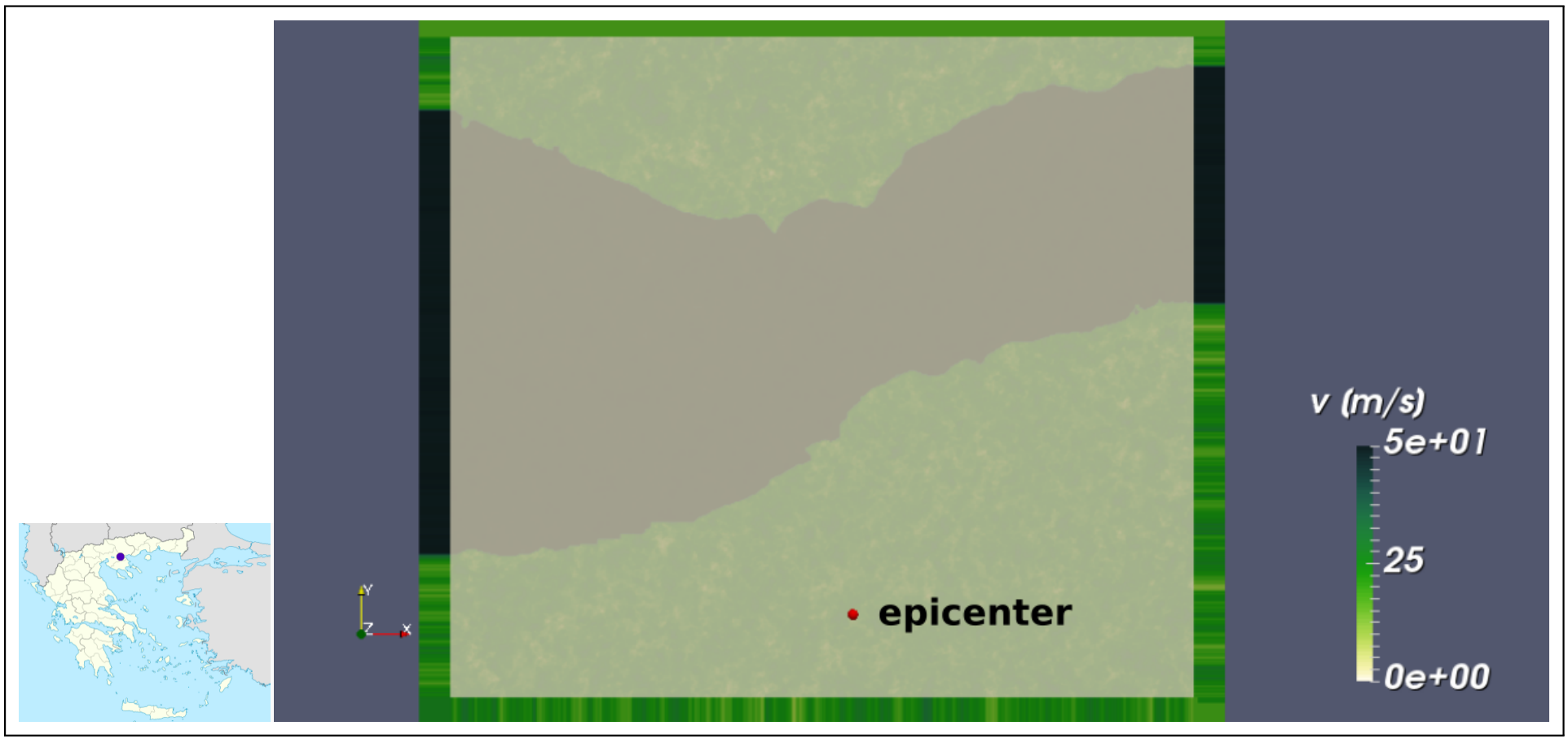


Figure – Earthquake simulation at the Volvi basin (Greece) [5]. 13 km × 11 km wide area. ≈7 h wall-time - 216 MPI cores @Ruche (≈62 days CPU time)

The earthquake engine : SEM3D

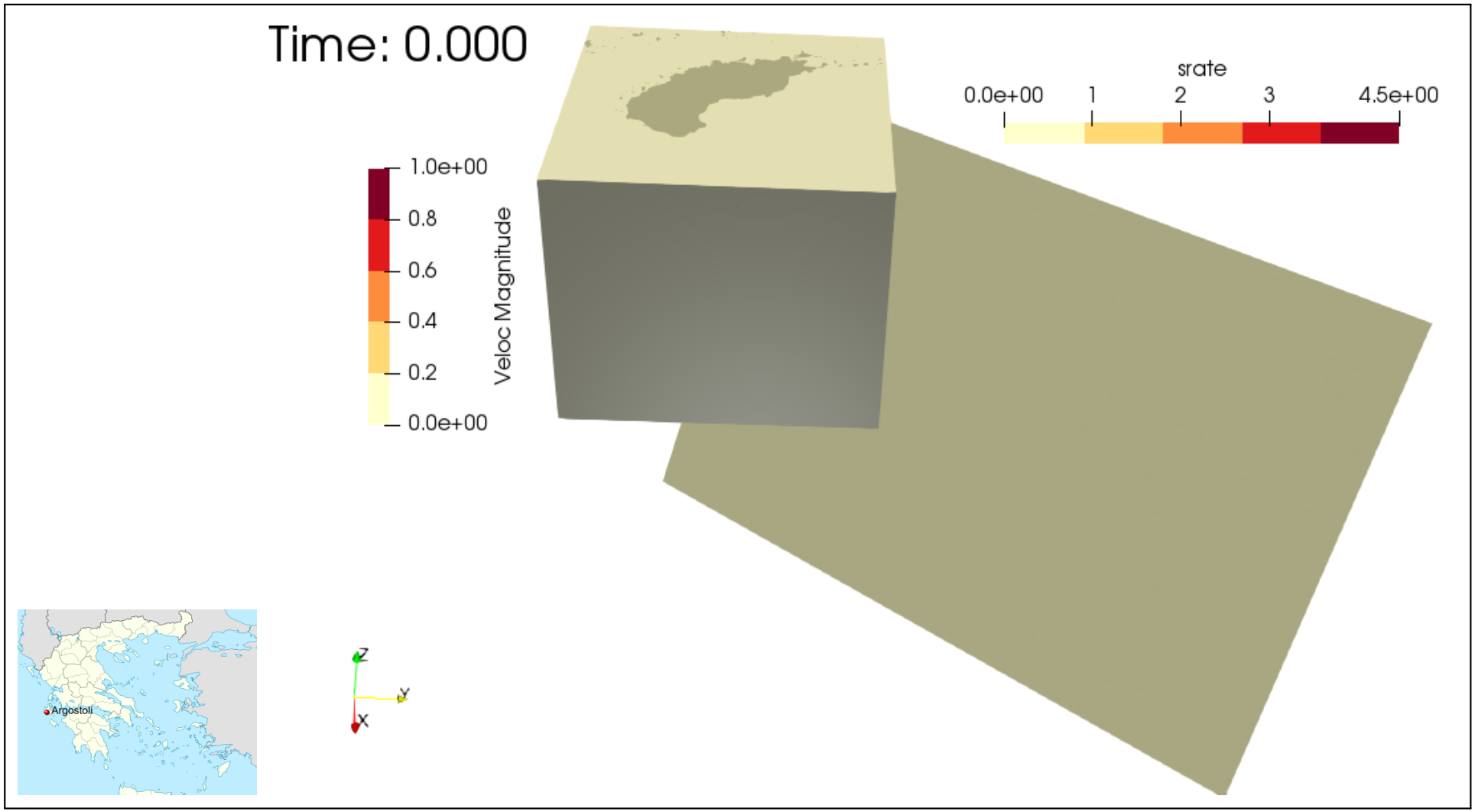
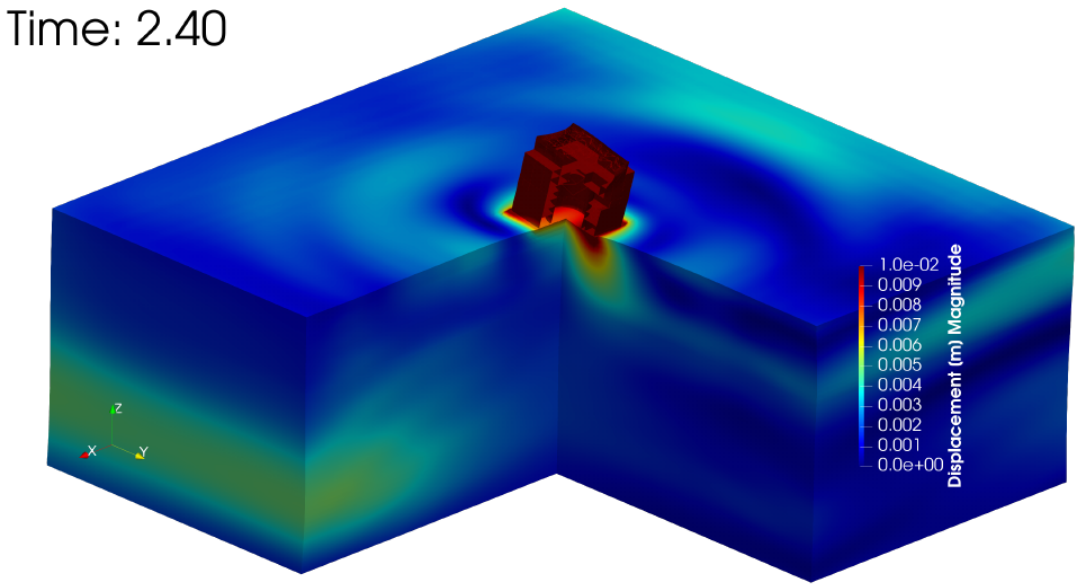


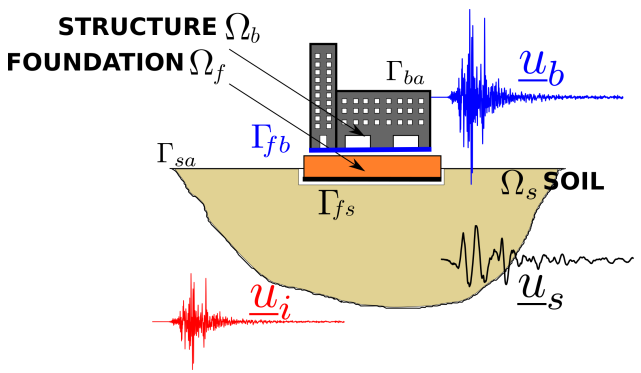
Figure – 1.3 $\cdot 10^{10}$ dofs ; 0-10 Hz Argostoli earthquake [10]. ≈20 h wall-time - 4000 MPI cores @Occigen (3333 days CPU time)

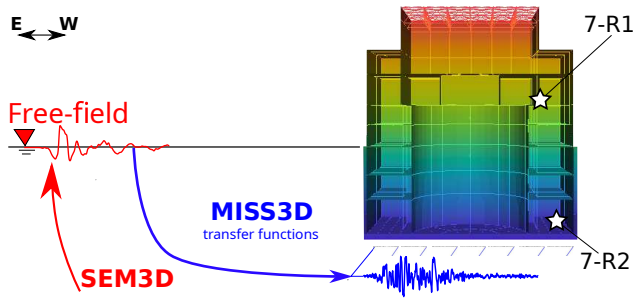
Earthquake simulation at several nuclear facilities

Kashiwazaki-Kariwa NPP (Japan) [6]



Weak-coupling with code_aster/Cast3M





Open questions

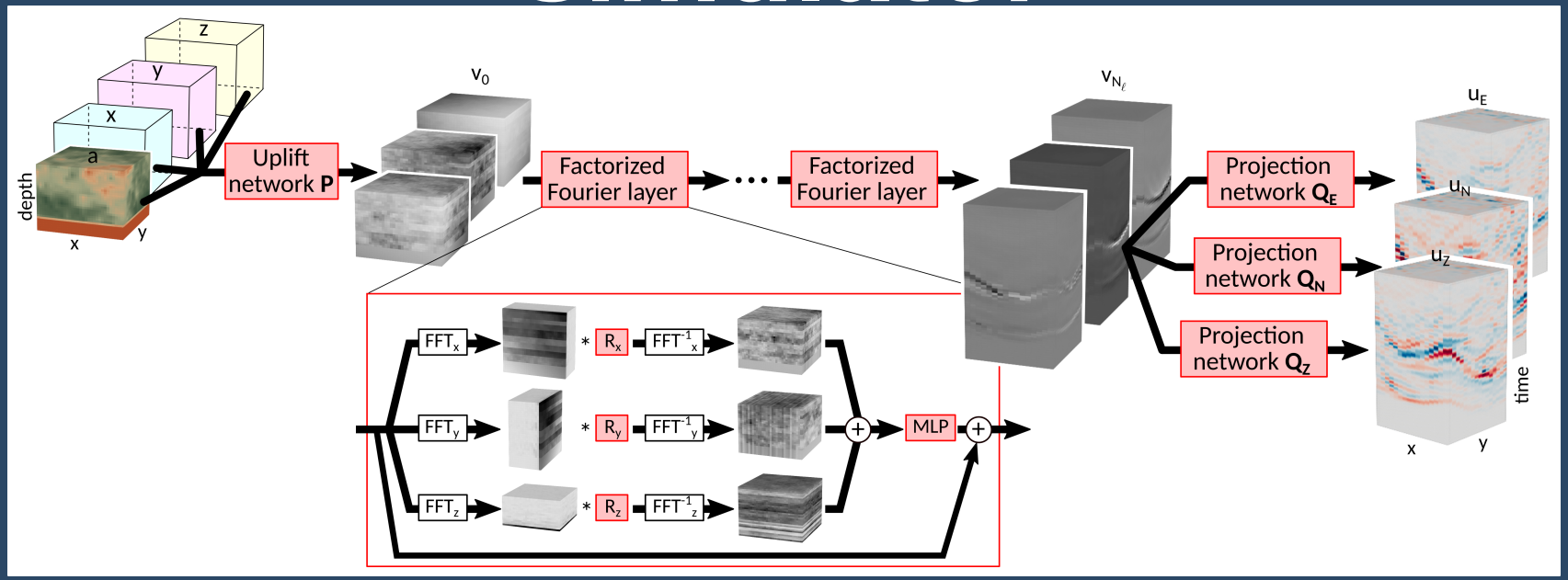
Summary

- Retro-engineering is hard but not impossible...
- ...in a limited frequency range (0-10 Hz)
- ...and with high uncertainty

But...

- **...what if multiple geological models are available ?**
- **...what if no observations are available ?**
- **...how to reduce the computational cost ?**
- **...how to simulate multiple scenarios REAL TIME ?**

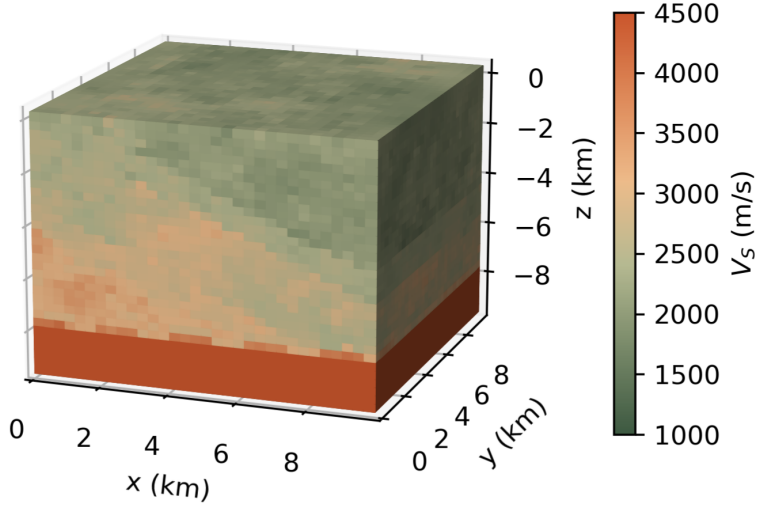
Earthquake neural simulator



Neural operators
for 3D wave equation

$(\mathcal{E} \subset \mathbb{R}^3, \mathcal{R} = (\mathbf{0}, \boldsymbol{i}_x, \boldsymbol{i}_y, \boldsymbol{i}_z))$

32× 32 × 32 voxels (300 m resolution)



- $\Omega =]0, L[^3 ; \partial\Omega_n := \{z = 0\}$
- Sommerfeld's radiation replaced by PML
- Random fluctuation of $\rho(\boldsymbol{x}), \lambda(\boldsymbol{x}), \mu(\boldsymbol{x})$ (`randomFields` [3])
- $c_S(\boldsymbol{x}) = \sqrt{\frac{\lambda+2\mu}{\rho}}$; $\frac{c_P}{c_S}(\boldsymbol{x}) = 1.7$ [9]
- $\boldsymbol{f} : (\boldsymbol{x}; t) \mapsto a(t)\boldsymbol{h}(\boldsymbol{x})$

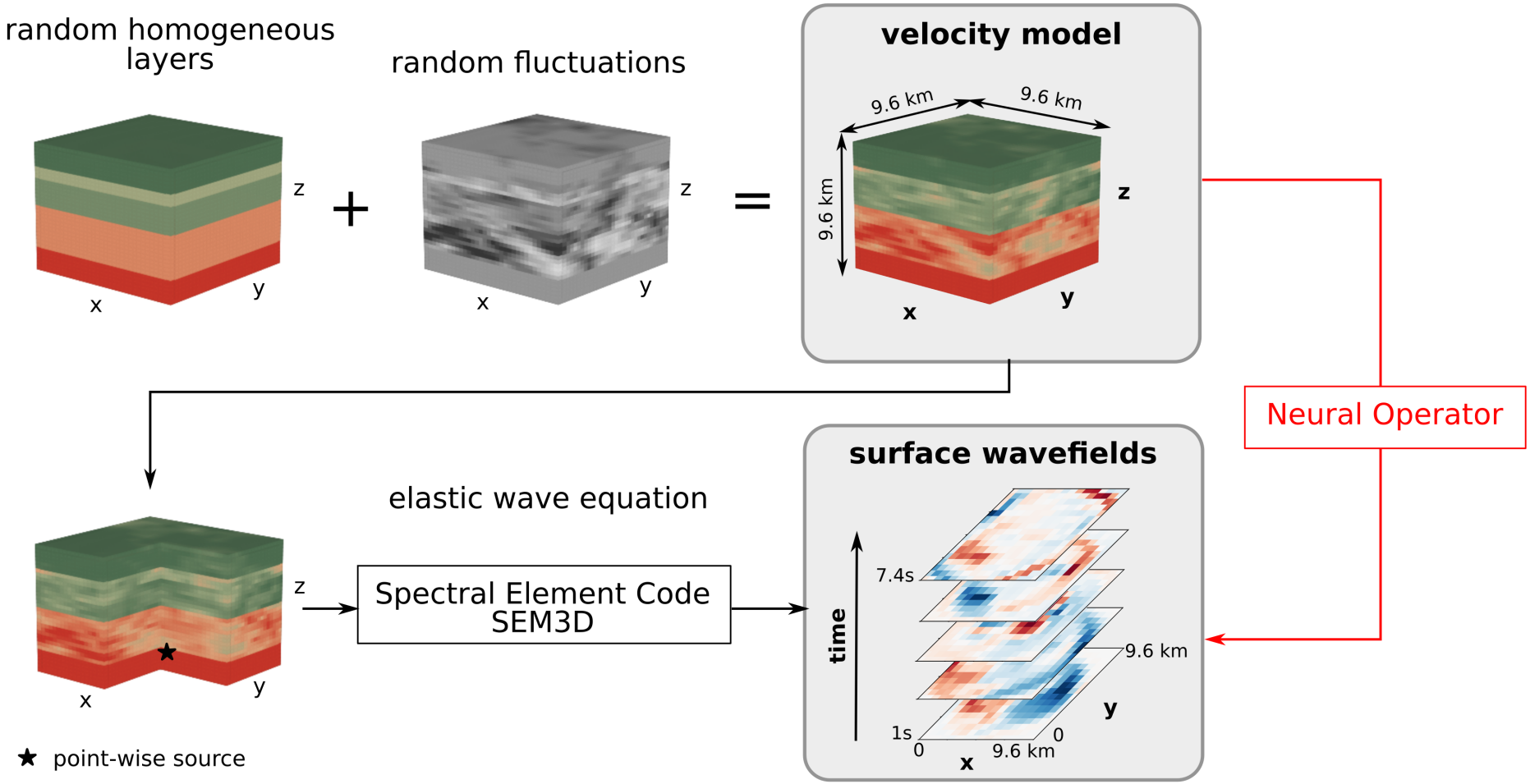
Green function $\boldsymbol{u}_G(\boldsymbol{x}, t; \boldsymbol{\xi}, \tau, \boldsymbol{i}_k) : \mathcal{D}_{c_S} \boldsymbol{u}_G = \delta_\tau(t)\, \delta_{\boldsymbol{\xi}}(\boldsymbol{x})\, \boldsymbol{i}_k$

$$\rho \partial^2_{tt} \boldsymbol{u}_G = (\lambda + 2\mu)\, \boldsymbol{\nabla}_{\boldsymbol{x}} \mathrm{div}_x(\boldsymbol{u}_G) + \mu \boldsymbol{\Delta}_{\boldsymbol{x}} \boldsymbol{u}_G + \boldsymbol{\nabla}_{\boldsymbol{x}} \lambda (\mathrm{div}_x(\boldsymbol{u}_G)) - \mu \boldsymbol{\nabla}_{\boldsymbol{x}} \wedge \boldsymbol{\nabla}_{\boldsymbol{x}} \wedge \boldsymbol{u}_G + \delta_\tau(t)\, \delta_{\boldsymbol{\xi}}(\boldsymbol{x})\, \boldsymbol{i}_k \quad (1)$$

Representation theorem with traction-free surface [1] :

$$\boldsymbol{u}(\boldsymbol{x}; t) = \sum_{k=1}^{3} \int_{\mathbb{R}} \int_{\Omega} \langle \boldsymbol{u}_G(\boldsymbol{x}, t-\tau; \boldsymbol{\xi}, 0, \boldsymbol{i}_k), \boldsymbol{h}(\boldsymbol{\xi}) \rangle a(\tau) \boldsymbol{i}_k + \sum_{k=1}^{3} \int_{\mathbb{R}} \int_{\partial\Omega} \boldsymbol{u}_G(\boldsymbol{x}, t-\tau; \boldsymbol{\xi}, 0, \boldsymbol{i}_k)\, \cancelto{0}{t_{n,k}(\boldsymbol{u}(\boldsymbol{\xi}, \tau))}$$

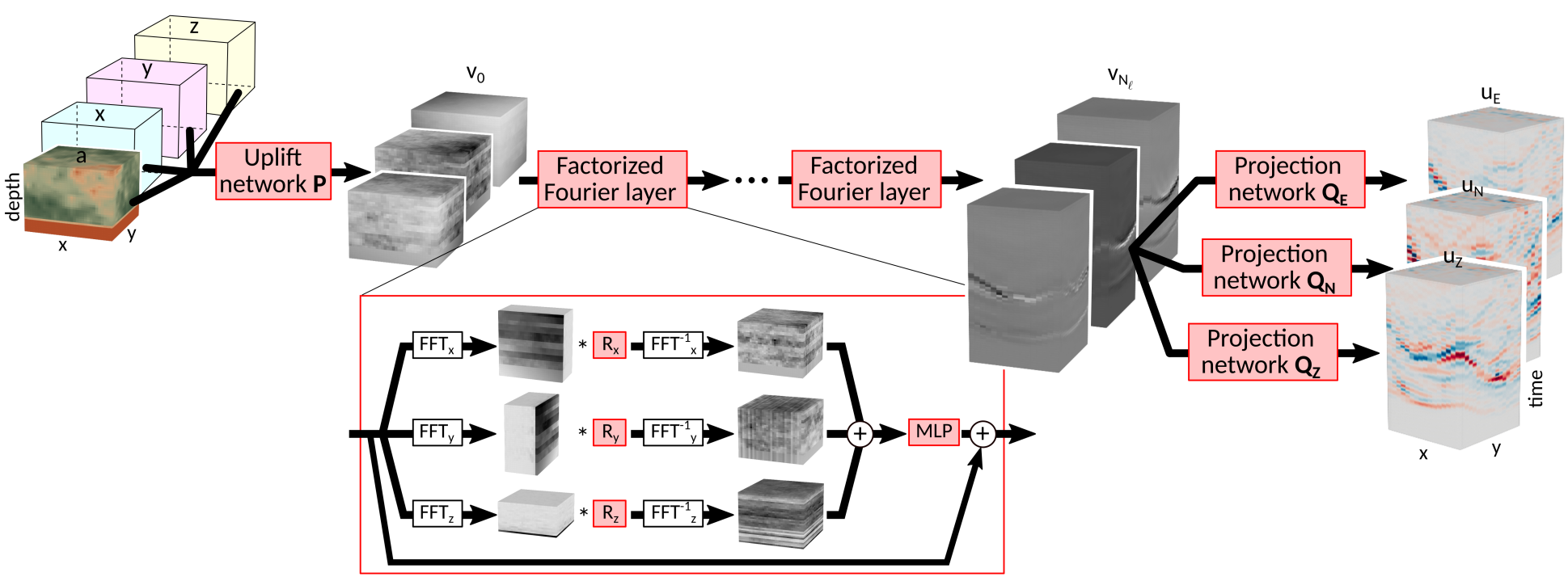
HEMEW-3D (link) : 30000+ SEM3D simulations at 5 Hz (open-source !)



Non-linear mapping $G : c_S \in L^2(\Omega) \mapsto \dot{\boldsymbol{u}} \in H_0^1(\mathbb{R}^+, H^1(\partial\Omega|_n)^3)$?

Neural operator $G_\theta(c_S)\boldsymbol{v} = \int_\Omega \mathbb{k}_\theta\left(\boldsymbol{x}, \boldsymbol{y}, c_S(\boldsymbol{x}), c_S(\boldsymbol{y})\right)\boldsymbol{v}(\boldsymbol{y})\, d\boldsymbol{y}$

(Factorized-) Fourier Neural Operators [11]
1. Iterative training

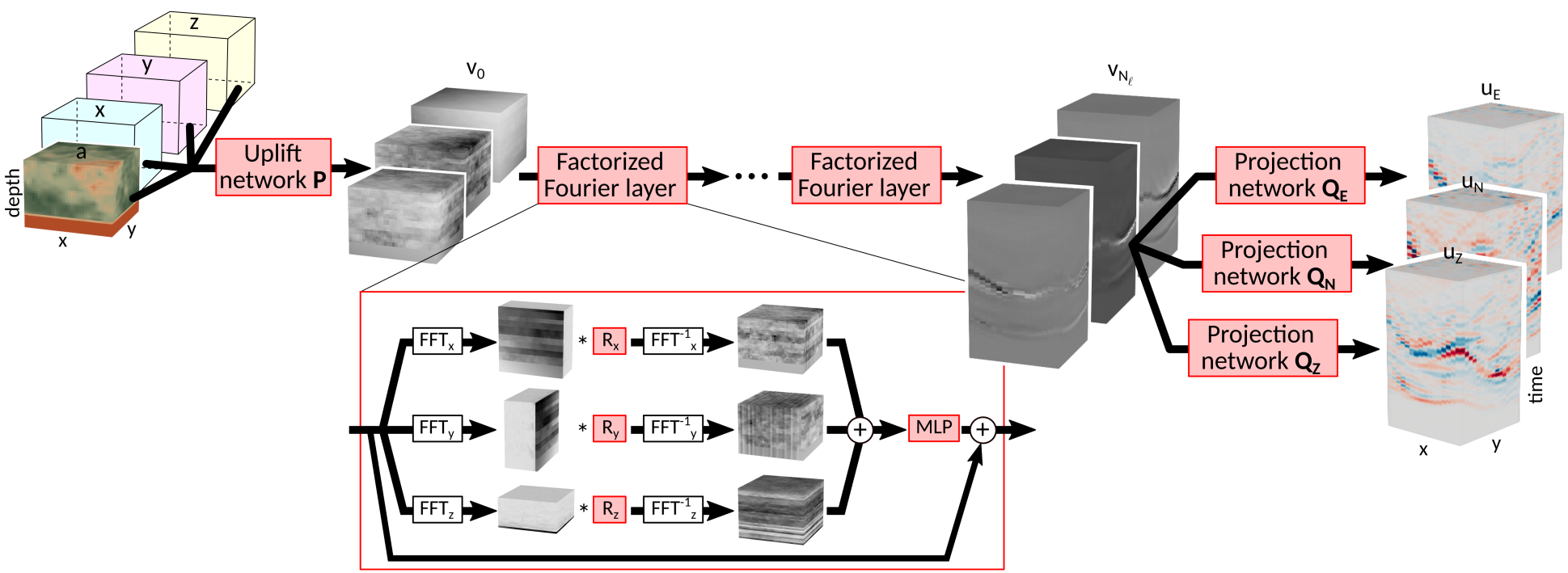


Fourier Neural Operators [8] :

1. Convolution theorem : $\mathbb{k}_{\boldsymbol{\theta}}\left(\boldsymbol{x}, \boldsymbol{y}, c_S\left(\boldsymbol{x}\right), c_S\left(\boldsymbol{y}\right)\right) = \mathbb{k}_{\boldsymbol{\theta}}\left(\boldsymbol{x} - \boldsymbol{y}\right)$
2. Iterative learning : $G_{\boldsymbol{\theta}} = Q \circ H_F^{(\ell)} \circ H_F^{(\ell-1)} \circ \ldots H_F^{(0)} \circ P$

$$\left(\boldsymbol{x}, c_S\left(\boldsymbol{x}\right)\right) = \boldsymbol{\xi} \rightarrow \boldsymbol{v}^{(0)}\left(\boldsymbol{\xi}\right) \rightarrow \ldots \boldsymbol{v}^{(\ell)} \rightarrow \ldots \boldsymbol{v}^{(\ell)} \rightarrow \dot{\boldsymbol{u}}\left(\boldsymbol{x}; t\right)|_{\partial\Omega_n}$$

(Factorized-) Fourier Neural Operators [11]
2. Neural-Network and Fast-Fourier Transform

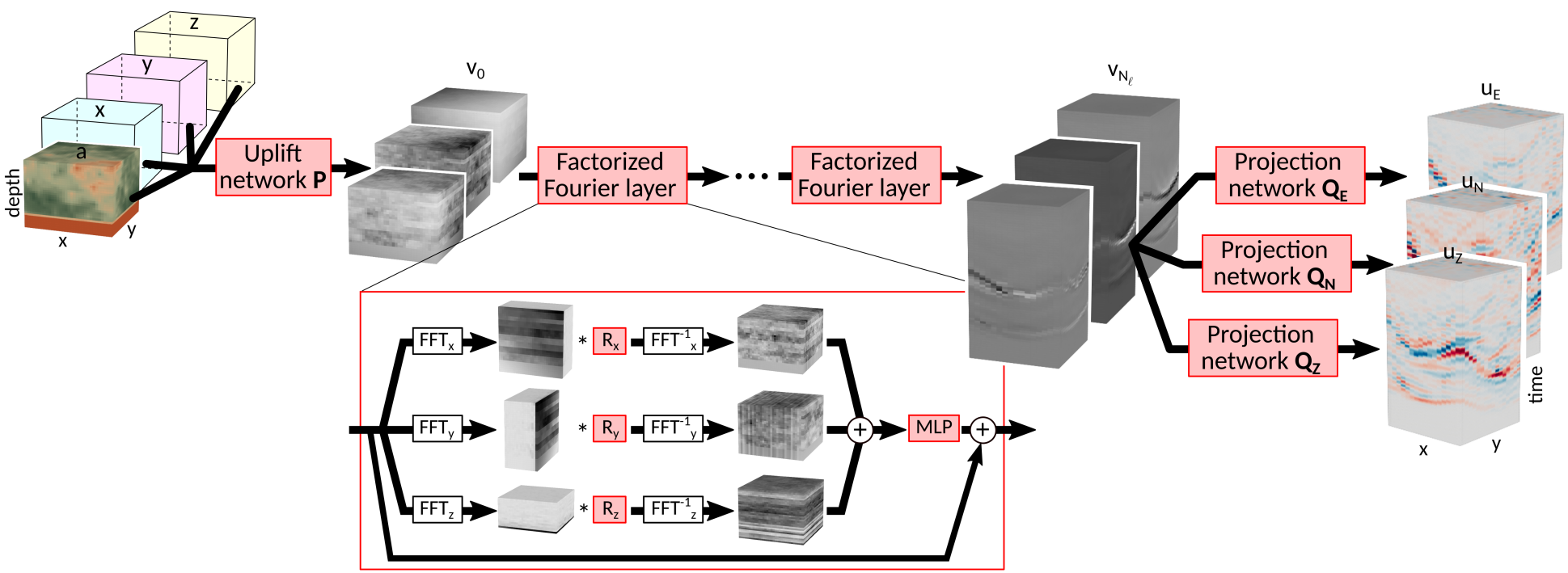


Fourier Neural Operators [8] :

4. Neural Network layer : $\boldsymbol{v}^{(\ell+1)} = \sigma\left(\boldsymbol{W}^{(\ell)}.\boldsymbol{v}^{(\ell)} + \int_\Omega \mathbb{k}^{(\ell)}\left(\boldsymbol{x},\boldsymbol{y}\right)\boldsymbol{v}^{(\ell)}\left(\boldsymbol{y}\right)d\boldsymbol{y}\right)$
5. Convolution in Fourier domain $\mathcal{R}^{(\ell)} := \mathcal{F}\left(\mathbb{k}^{(\ell)}\right)$ $\quad \#\boldsymbol{\theta} : O(M^{(\ell)}_{(1)} M^{(\ell)}_{(2)} M^{(\ell)}_{(3)})$

$$\boldsymbol{v}^{(\ell+1)}\left(\boldsymbol{\xi}\right) = \sigma\left(\mathcal{F}^{-1}\left(\mathcal{R}^{(\ell)} \odot \mathcal{F}\left(\boldsymbol{v}^{(\ell)}\right)\left(\boldsymbol{\xi}\right)\right) + \boldsymbol{W}^{(\ell)}\boldsymbol{v}^{(\ell)}\left(\boldsymbol{\xi}\right) + \boldsymbol{b}^{(\ell)}\right) \quad (2)$$

(Factorized-) Fourier Neural Operators [11]
3. Factorization



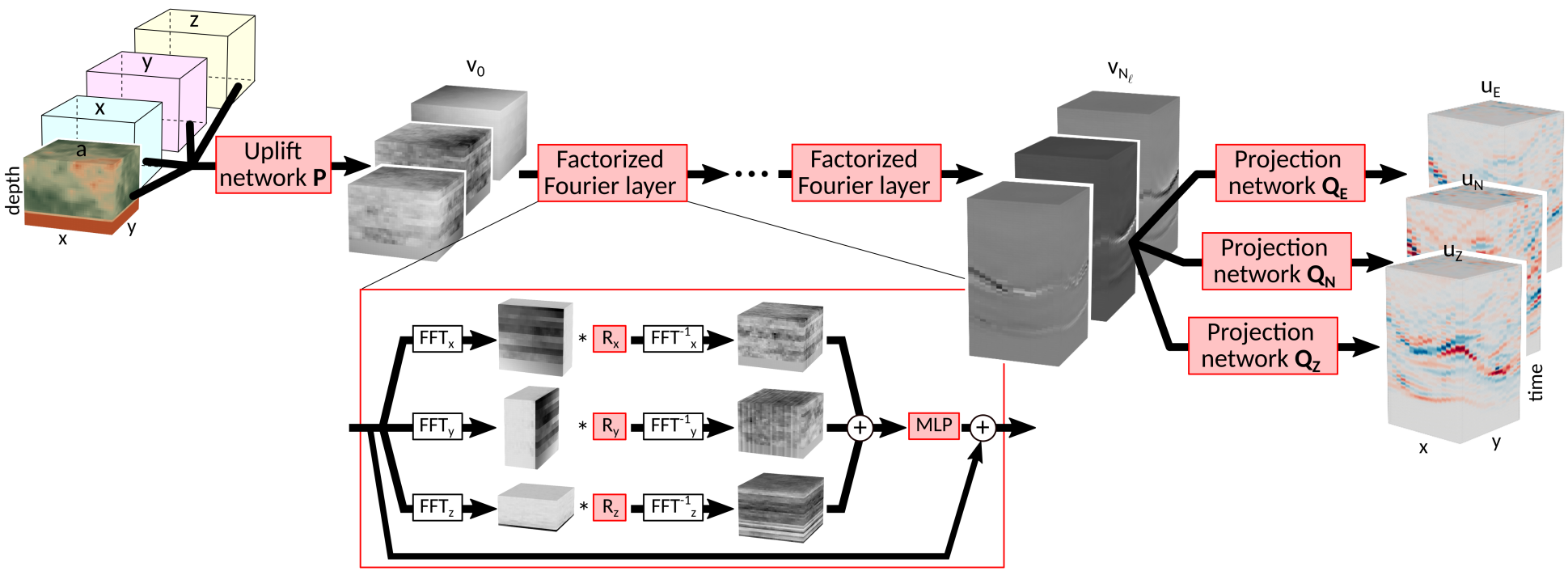
Factorized Fourier Neural Operators [11] :

6. Three 1D FFTs instead of a single 3D FFT

$$\#\boldsymbol{\theta} : \mathcal{O}\left(M_{(1)}^{(\ell)} + M_{(2)}^{(\ell)} + M_{(3)}^{(\ell)}\right) \text{ per layer)}$$

$$\boldsymbol{v}^{(\ell+1)}(\boldsymbol{\xi}) = \boldsymbol{v}^{(\ell)}(\boldsymbol{\xi}) + \sigma\left[\boldsymbol{W}_2^{(\ell)}\ \sigma\left(\boldsymbol{W}_1^{(\ell)}\ \mathcal{K}^{(\ell)}(\boldsymbol{v}^{(\ell)})(\boldsymbol{\xi}) + \boldsymbol{b}_1^{(\ell)}\right) + \boldsymbol{b}_2^{(\ell)}\right] \tag{3}$$

$$\mathcal{K}^{(\ell)}(\boldsymbol{v}^{(\ell)}) = \mathcal{F}_{(1)}^{-1}\left(\mathcal{R}_{(1)}^{(\ell)}\mathcal{F}_{(1)}(\boldsymbol{v}^{(\ell)})\right) + \mathcal{F}_{(2)}^{-1}\left(\mathcal{R}_{(2)}^{(\ell)}\mathcal{F}_{(2)}(\boldsymbol{v}^{(\ell)})\right) + \mathcal{F}_{(3)}^{-1}\left(\mathcal{R}_{(3)}^{(\ell)}\mathcal{F}_{(3)}(\boldsymbol{v}^{(\ell)})\right) \tag{4}$$



Factorized Fourier Neural Operators [11] :

7. Uplift sub-network
   $P : (x, y, z, c_S(x, y, z)) \in \mathbb{R}^4 \mapsto MLP_2(MLP_1(x, y, z, c_S(x, y, z))) \in \mathbb{R}^{d_v}$
8. Projection sub-networks $Q_i : \boldsymbol{v}^{N_\ell} \mapsto MLP_2(MLP_1(\boldsymbol{v}^{N_\ell}))$ (projection of d_v-channel variable $\boldsymbol{v}^{N_\ell}$ onto 1-channel physical variables $\dot{\boldsymbol{u}}_i(t)$

(Factorized-) Fourier Neural Operators [11]
applied to seismology [7]

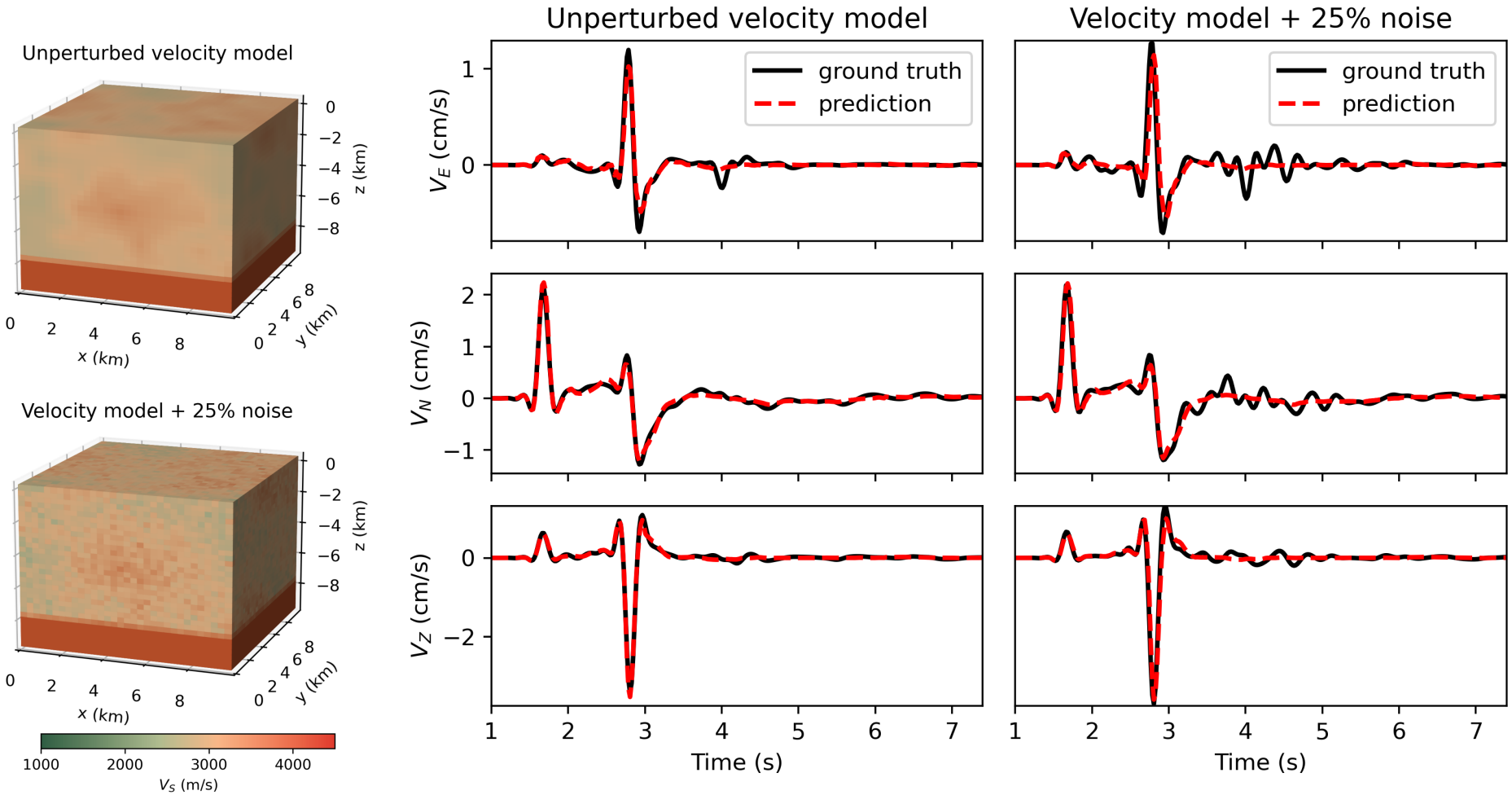


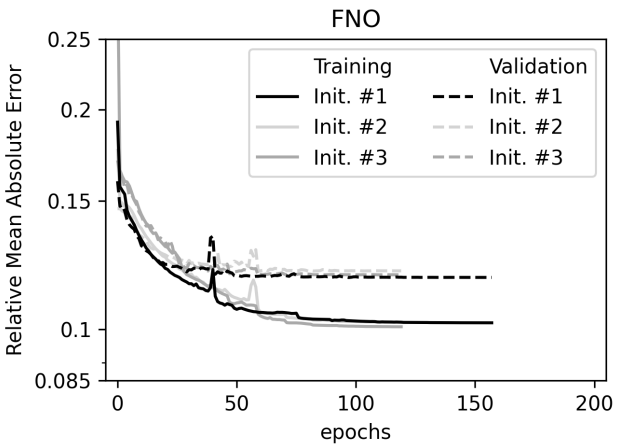
Figure – Robustness to noise [7].

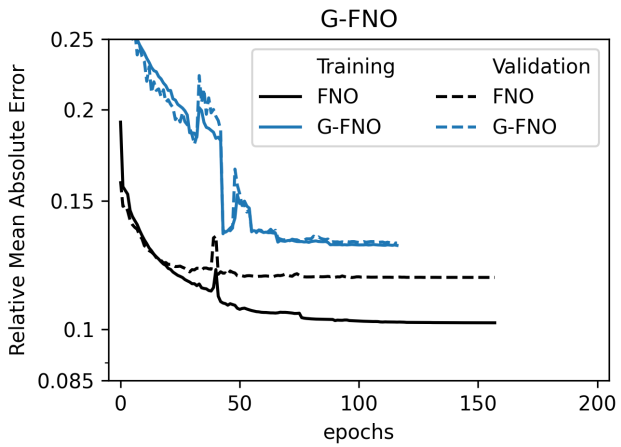
F-FNO elastodynamics benchmark [7]

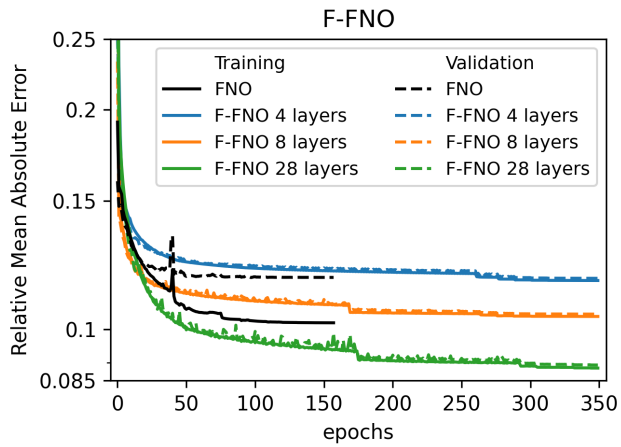
4 Nvidia Ampere A100 GPUs. $d_v = 16$, $M^{(\ell)}_{(1)} = M^{(\ell)}_{(2)} = 16, \forall \ell$, $M^{(1)}_{(3)} = 16$, $M^{(\ell)}_{(3)} = 32, \forall \ell \geq 2$

Model	d_Θ	$\frac{1}{Ne}\sum_{e=1}^{Ne} t_{tr}(e)$ (s)	t_i ($\times 10^{-3}$ s)	Speed-up CPU/GPU ($\times 10^7$)
FNO	**58.7m**	**129**	**5.0**	**1.6**
U-NO	24.6m	216	6.3	1.3
G-FNO	**67.2m**	**690**	**4.0**	**2.0**
F-FNO $N^{(\ell)}$ =4	139k	216	3.0	2.7
F-FNO $N^{(\ell)}$ =8	**246k**	**222**	**3.3**	**2.5**
F-FNO $N^{(\ell)}$ =12	353k	225	3.7	2.2
F-FNO $N^{(\ell)}$ =16	460k	231	4.3	1.9
F-FNO $N^{(\ell)}$ =20	568k	246	4.7	1.7
F-FNO $N^{(\ell)}$ =24	675k	273	5.0	1.6
F-FNO $N^{(\ell)}$ =28	**782k**	**300**	**5.3**	**1.5**

Table – F-FNO benchmark on $\eta = 0.0006$. The speed-up is computed as the ratio between the mean simulation time (**22.72 h CPU equiv.**) and the inference time [7].



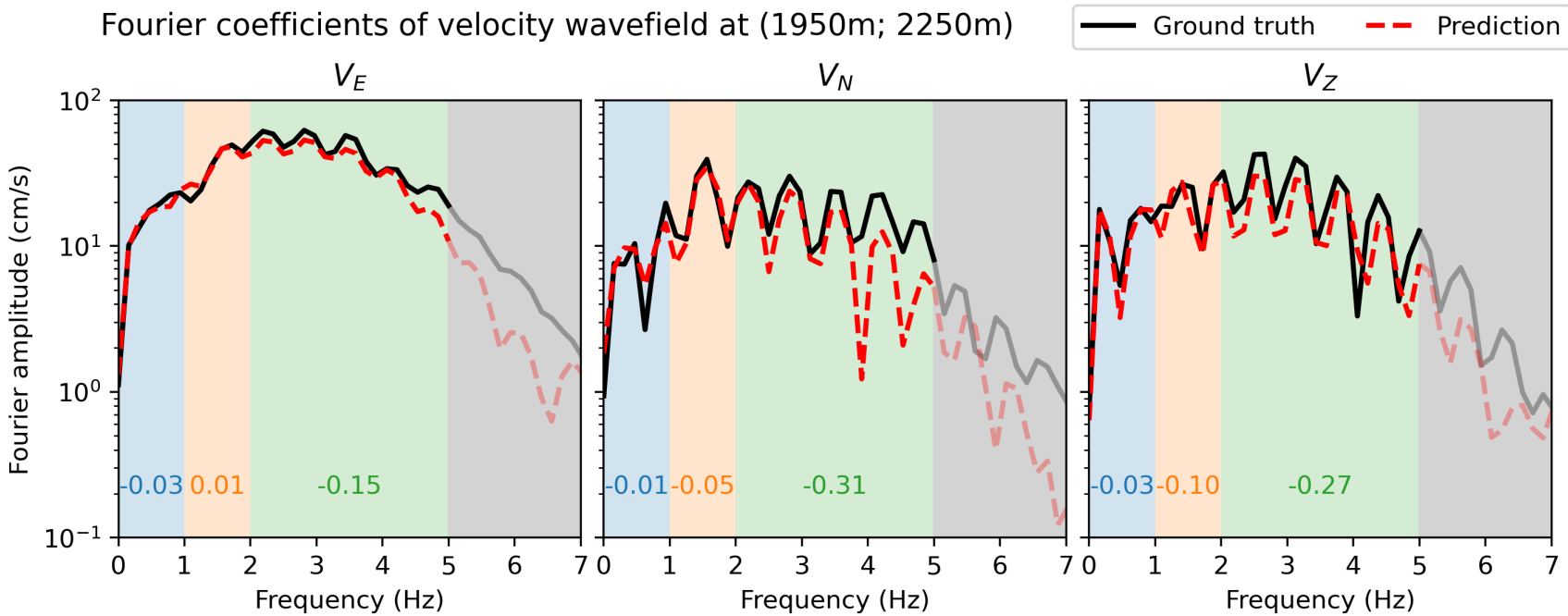




F-FNO Benchmark
Some comparisons in terms of metrics.

Model	rRMSE	$rFFT_{low}$	$rFFT_{mid}$	$rFFT_{high}$
FNO	**0.23 ± 0.088**	**-0.17 ± 0.18**	**-0.30 ± 0.24**	**-0.44 ± 0.30**
U-NO	0.22 ± 0.088	-0.16 ± 0.16	-0.28 ± 0.22	-0.44 ± 0.28
G-FNO	**0.26 ± 0.073**	**-0.53** ± 0.12	**-0.76 ± 0.11**	**-0.94 ± 0.04**
F-FNO $N^{(\ell)}$ =4	0.23 ± 0.081	-0.29 ± 0.16	-0.42 ± 0.21	-0.55 ± 0.26
F-FNO $N^{(\ell)}$ =8	0.21 ± 0.083	-0.15 ± 0.14	-0.26 ± 0.19	-0.37 ± 0.26
F-FNO $N^{(\ell)}$ =28	**0.17 ± 0.081**	**-0.08 ± 0.10**	**-0.14 ± 0.15**	**-0.23 ± 0.22**

Table – Mean and standard deviation of relative biases for 1000 validation samples. $rFFT_{low}$, $rFFT_{mid}$, $rFFT_{high}$: frequency biases/deviations [7].



F-FNO elastodynamics
Parametric analysis

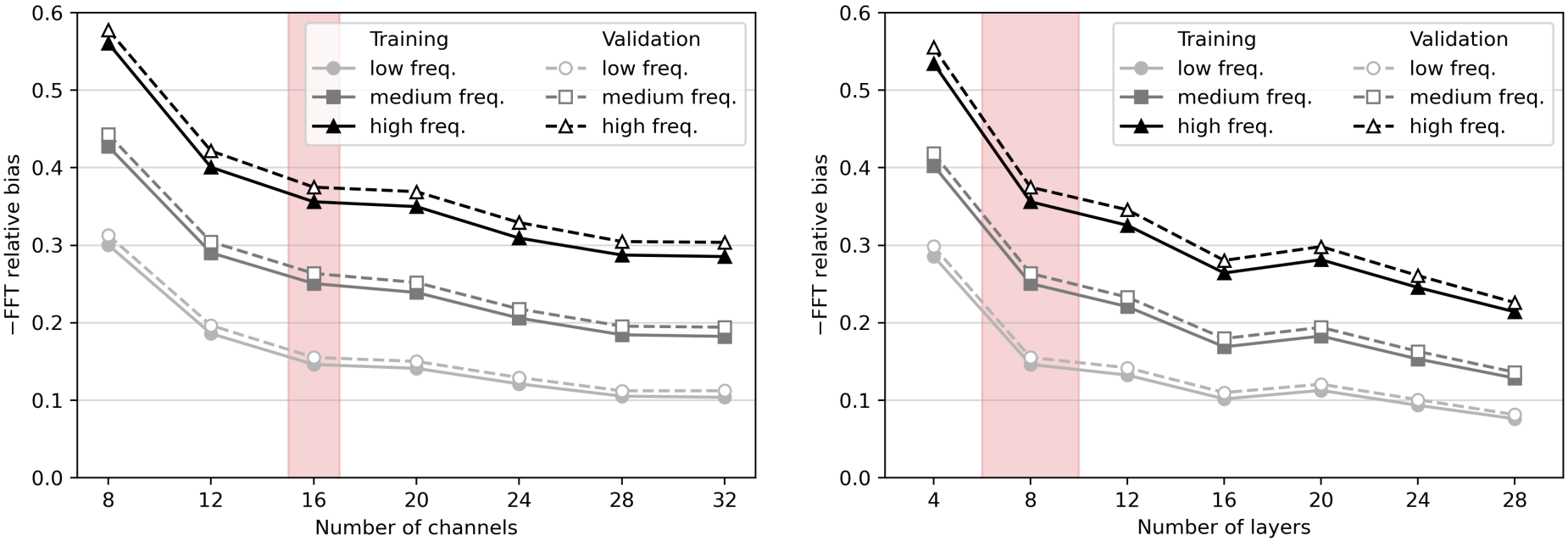


Figure – Left : effect of d_v ; right : effect of $N^{(\ell)}$ [7].

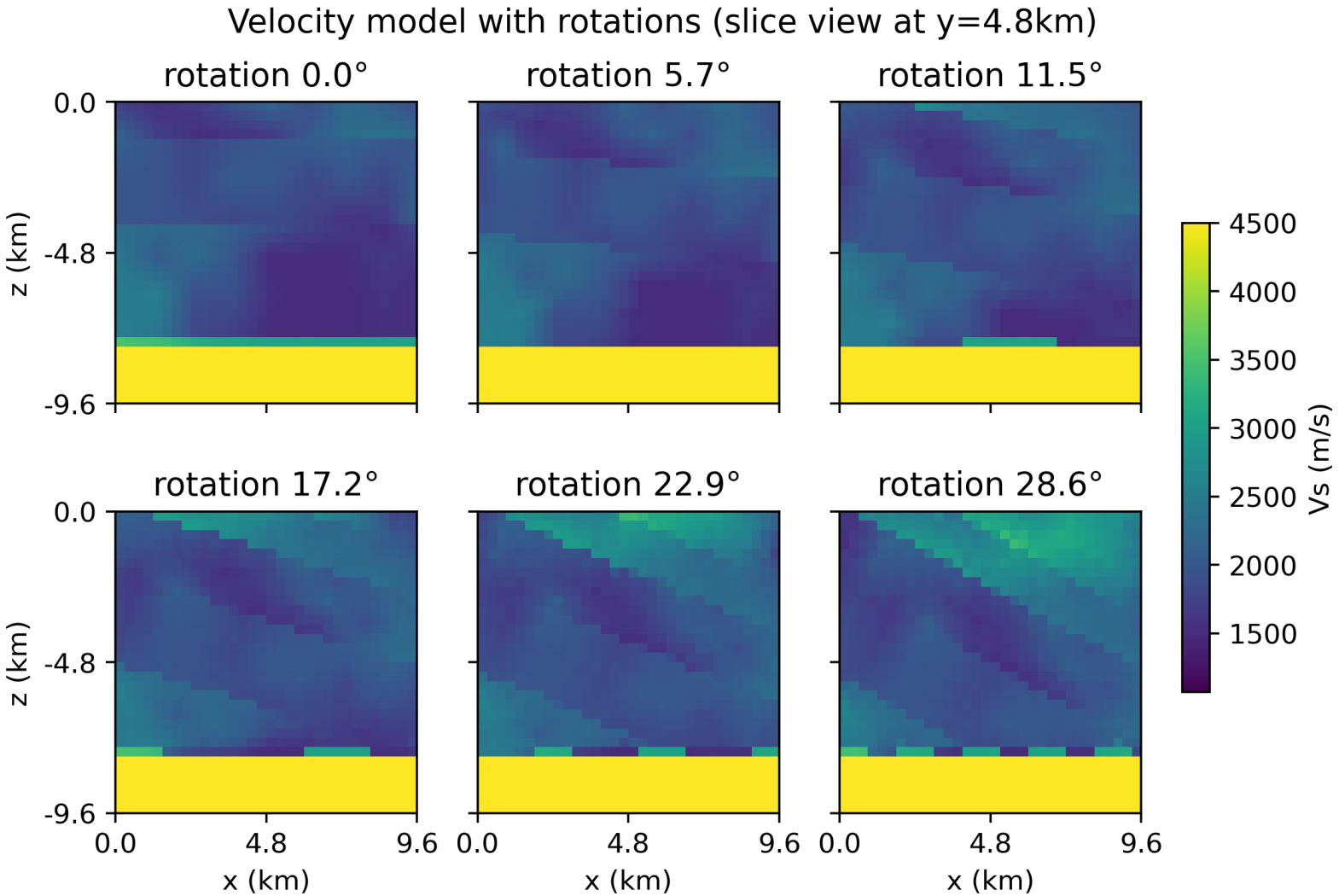


Figure – Rotating horizontal layers around the y-axis with five rotation angles (5.7°, 11.5°, 17.2°, 22.9°, and 28.6°) in x-z plane [7].

F-FNO elastodynamics
Out-of-distribution generalization

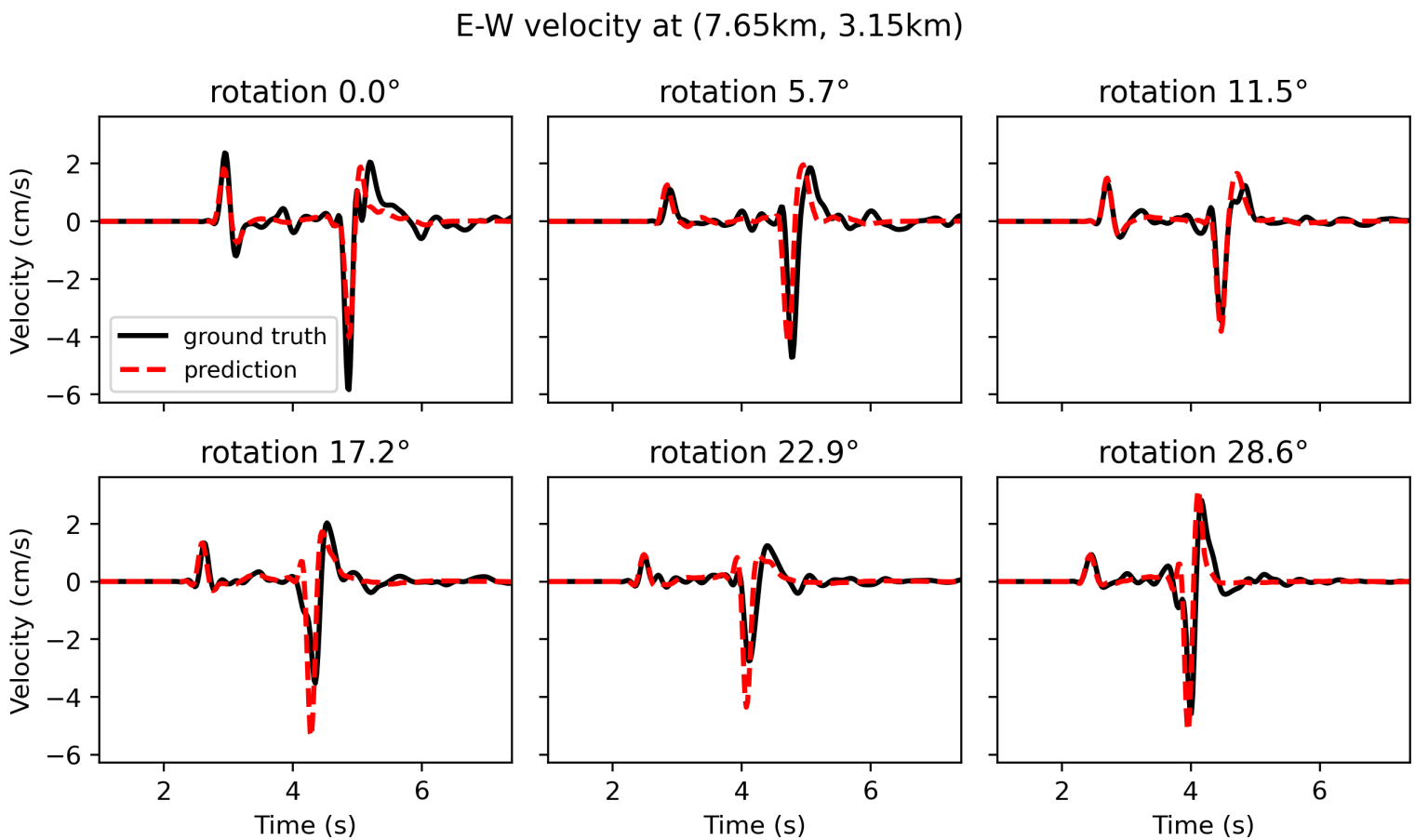


Figure – Rotating horizontal layers around the y-axis with five rotation angles (5.7°, 11.5°, 17.2°, 22.9°, and 28.6°). Corresponding time-histories [7].

Discrete operators are resolution-invariant ?

$$g(\Psi', \Phi') = T^{\dagger}_{\Phi'} \circ T_{\Phi} \circ g(\Psi, \Phi) \circ T^{\dagger}_{\Psi} \circ T_{\Psi'} \Longrightarrow \tau(\Psi, \Phi, \Psi', \Phi') = 0$$

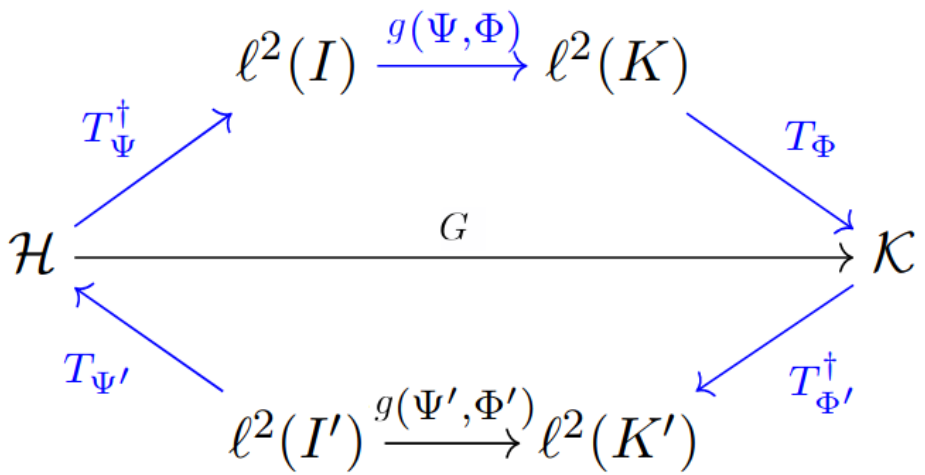


Figure – Representation equivalent Neural Operator (ReNO) [2]

On the representation equivalence[2]
Fourier Neural Operator

Fourier layer $\boldsymbol{v}^{(\ell+1)} = H_F^{(\ell)} \boldsymbol{v}^{(\ell)}$:

$$\boldsymbol{v}^{(\ell+1)}\left(\boldsymbol{\xi}\right) = \sigma\left(\mathcal{F}^{-1}\left(\mathcal{R}^{(\ell)} \odot \mathcal{F}\left(\boldsymbol{v}^{(\ell)}\right)\left(\boldsymbol{\xi}\right)\right) + \boldsymbol{W}^{(\ell)}\boldsymbol{v}^{(\ell)}\left(\boldsymbol{\xi}\right) + \boldsymbol{b}^{(\ell)}\right) \tag{5}$$

To simplify ($\boldsymbol{W}^{(\ell)} = \boldsymbol{0}, \boldsymbol{b}^{(\ell)} = \boldsymbol{0}$) [8]

- Fourier layer : $G = \sigma\left(K^{(\ell)}\boldsymbol{v}^{(\ell)}\left(\boldsymbol{\xi}\right)\right) = \sigma\left(\mathcal{F}^{-1}\left(\mathcal{R}^{(\ell)} \odot \mathcal{F}\left(\boldsymbol{v}^{(\ell)}\right)\left(\boldsymbol{\xi}\right)\right)\right)$
  - $\mathcal{F} : w \in L^2(\mathbb{T}) \mapsto \left\{\left\langle w, {}^{i\pi k\cdot}\right\rangle\right\}_{k\in\mathbb{Z}} \in \ell^2(\mathbb{Z})$
  - $\mathcal{F}^{-1} : \{W_k\}_{k\in\mathbb{Z}} \in \ell^2(\mathbb{Z}) \mapsto \sum_{k\in\mathbb{Z}} W_k e^{i\pi kx}$
- Discretization (F, F^{-1} : DFT) :
  $g = \sigma\left(k^{(\ell)}\boldsymbol{v}^{(\ell)}\left(\boldsymbol{\xi}\right)\right) = \sigma\left(F^{-1}\left(R^{(\ell)} \odot F\left(\boldsymbol{v}^{(\ell)}\right)\left(\boldsymbol{\xi}\right)\right)\right)$
- CDE : $K > 0, \mathcal{P}_K := \left\{w(x) = \sum_{k=-K}^{K} W_K e^{i\pi kx}, \{W_k\}_{k=-K}^{K} \in \mathbb{C}^{2K+1}\right\} \subset \mathcal{B}_{\frac{K}{2}}$:

$$\mathcal{P}_K \ni w = \sum_{k=-K}^{K} w\left(\frac{k}{2K+1}\right)\Psi_k(\cdot), \quad \Psi_K = \left\{\frac{1}{\sqrt{2(2K+1)}} d\left(\cdot - \frac{2k}{2K+1}\right)\right\}_{k=0}^{2K}$$

d =Dirac's kernel and DFT coefficients $\hat{W}_k = (2K+1)W_k, k \in \{-K \dots K\}$

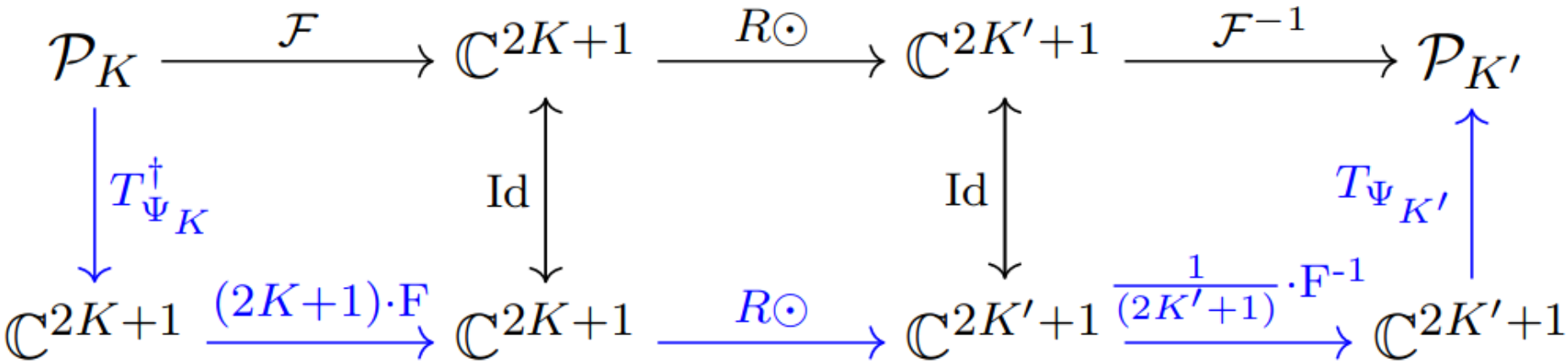


Figure – CDE for FNO. Reprinted from Bartolucci et al. [2].

- Representation equivalence : $K^{'} \leq K$
- Kernel weights $\{R_k\}_{k-=-K'}^{K'}$
- FNO (without activation) is a ReNO between bandlimited 2-periodic functions

$$(\mathcal{R} \odot \mathcal{F} w)(k) = R_k W_k, \quad k \in \left\{-K^{'}, \ldots, K^{'}\right\}$$

Activation function hampers CDE

$$\sigma(f) = ReLU(f) \notin \mathcal{P}_K$$

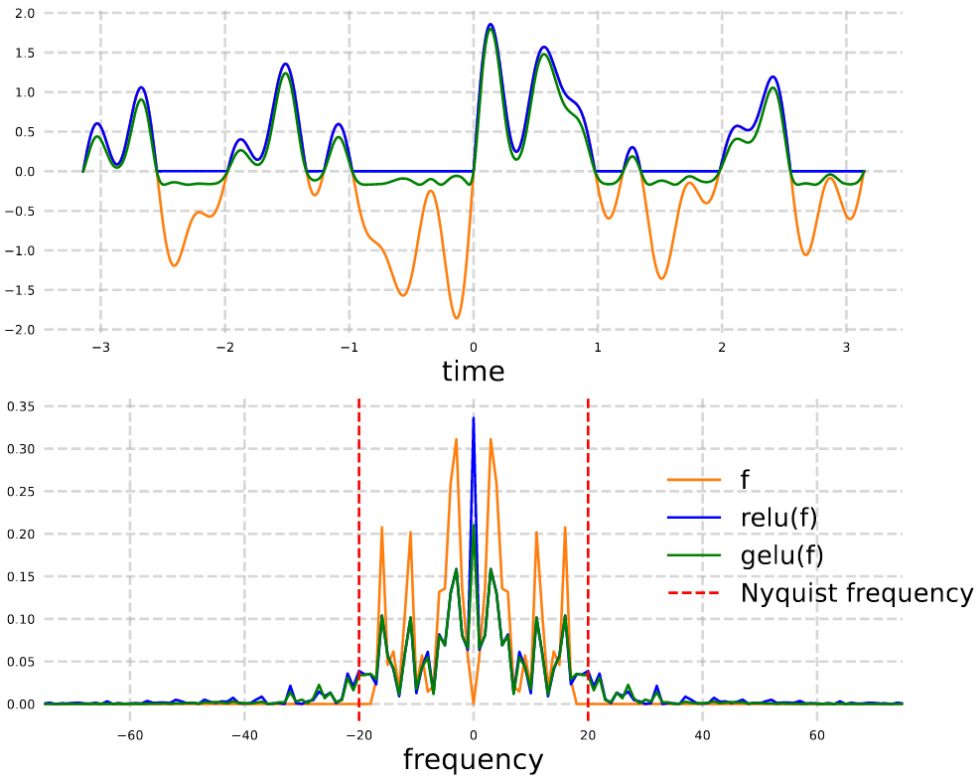
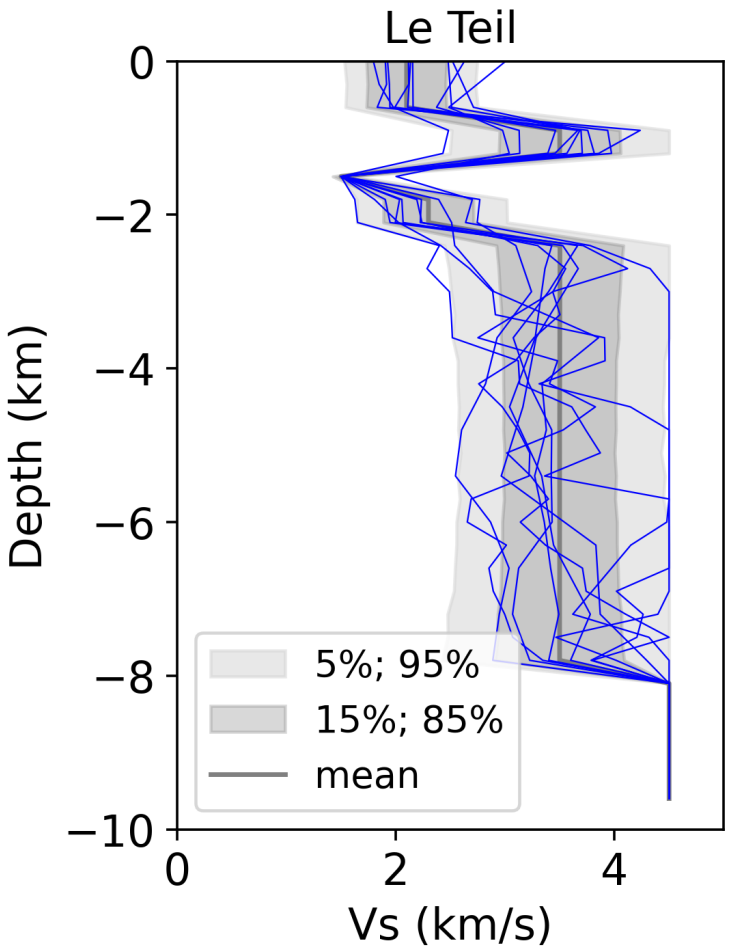


Figure – Activation function hampers CDE for FNO. Reprinted from Bartolucci et al. [2].

F-FNO elastodynamics
Transfer learning on Le Teil geology



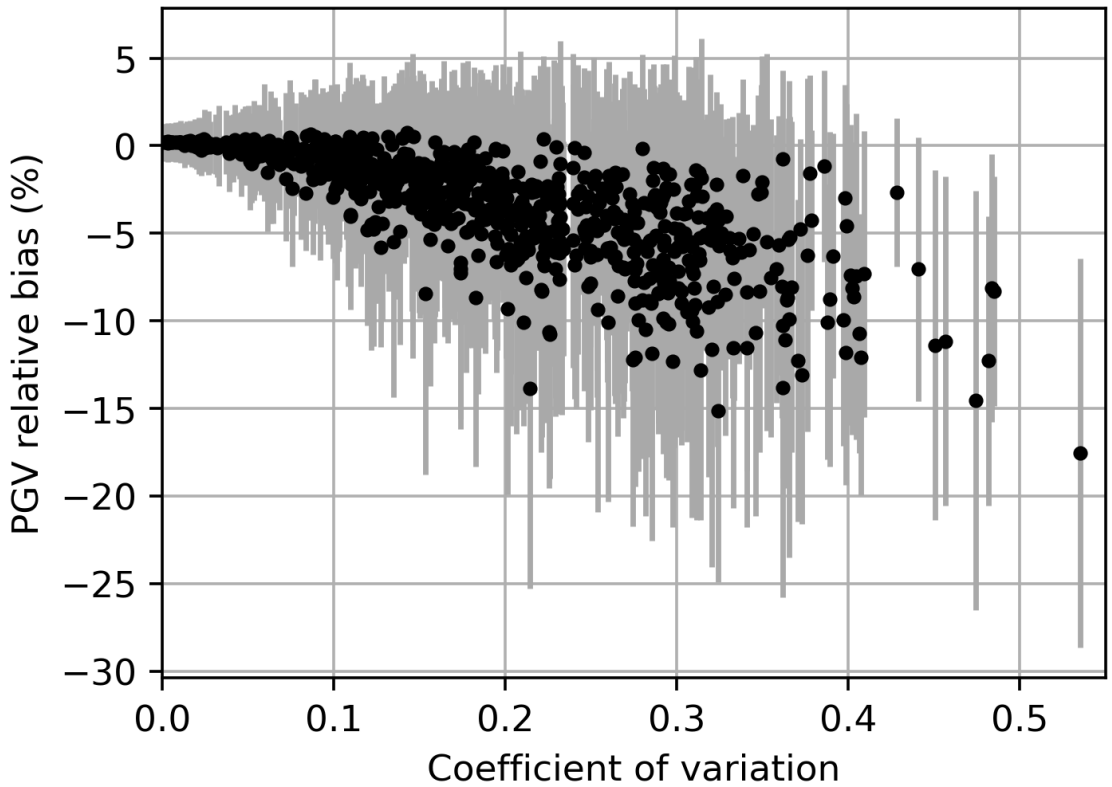
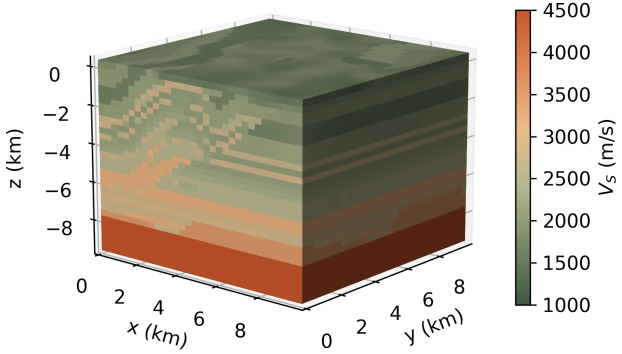
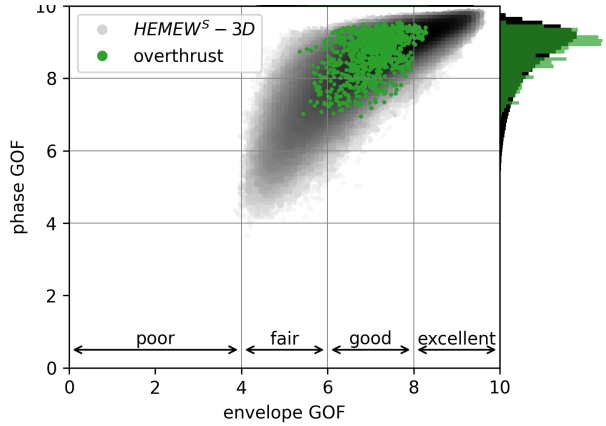


Figure – Transfer learning on Le Teil geology (left) for the 2019 M_W4.9 earthquake. Right : PGV relative bias as a function of the geology CoV.

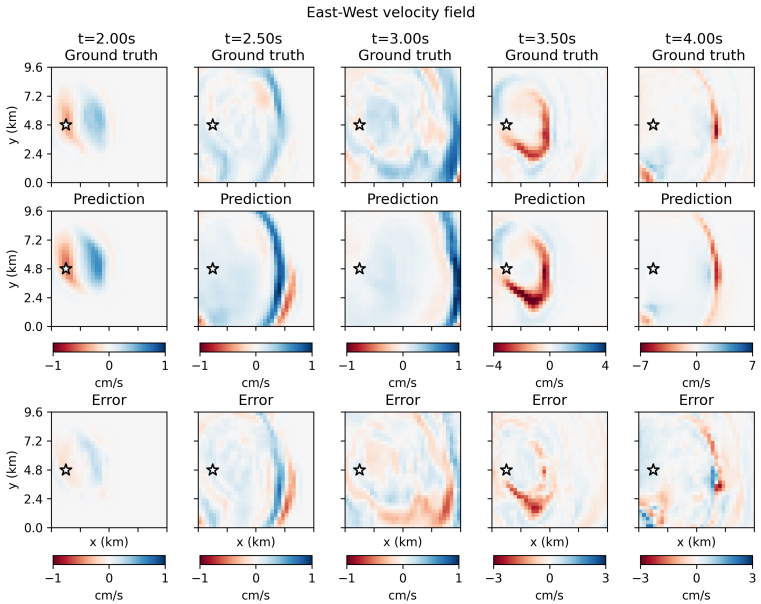
Transfer learning on complex setups



a



b



c

Multiple-Input Fourier Neural Operator (MIFNO)

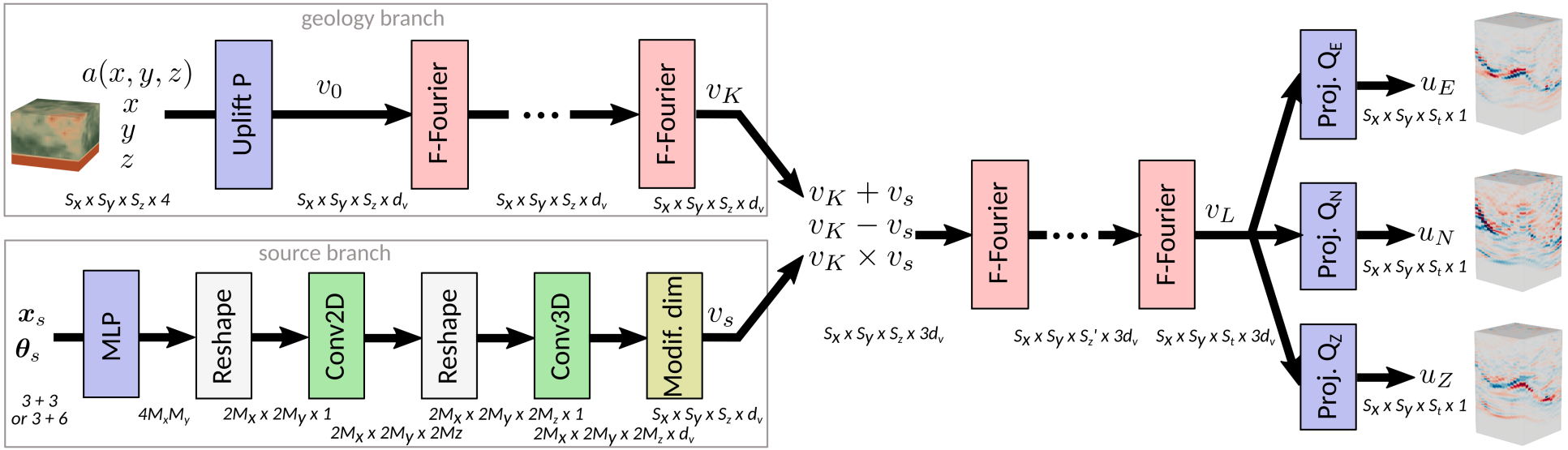


Figure – The MIFNO is made of a *geology branch* that encodes the geology with factorized Fourier (F-Fourier) layers, and a *source branch* that transforms the vector of source parameters $(\boldsymbol{x}_S, \boldsymbol{\theta}_S)$ into a 4D variable v_S matching the dimensions of the *geology branch* output v_K. Outputs of each branch are concatenated after elementary mathematical operations and the remaining factorized Fourier layers are applied. Uplift P and projection Q_E, Q_N, Q_Z blocks are the same as in the F-FNO.

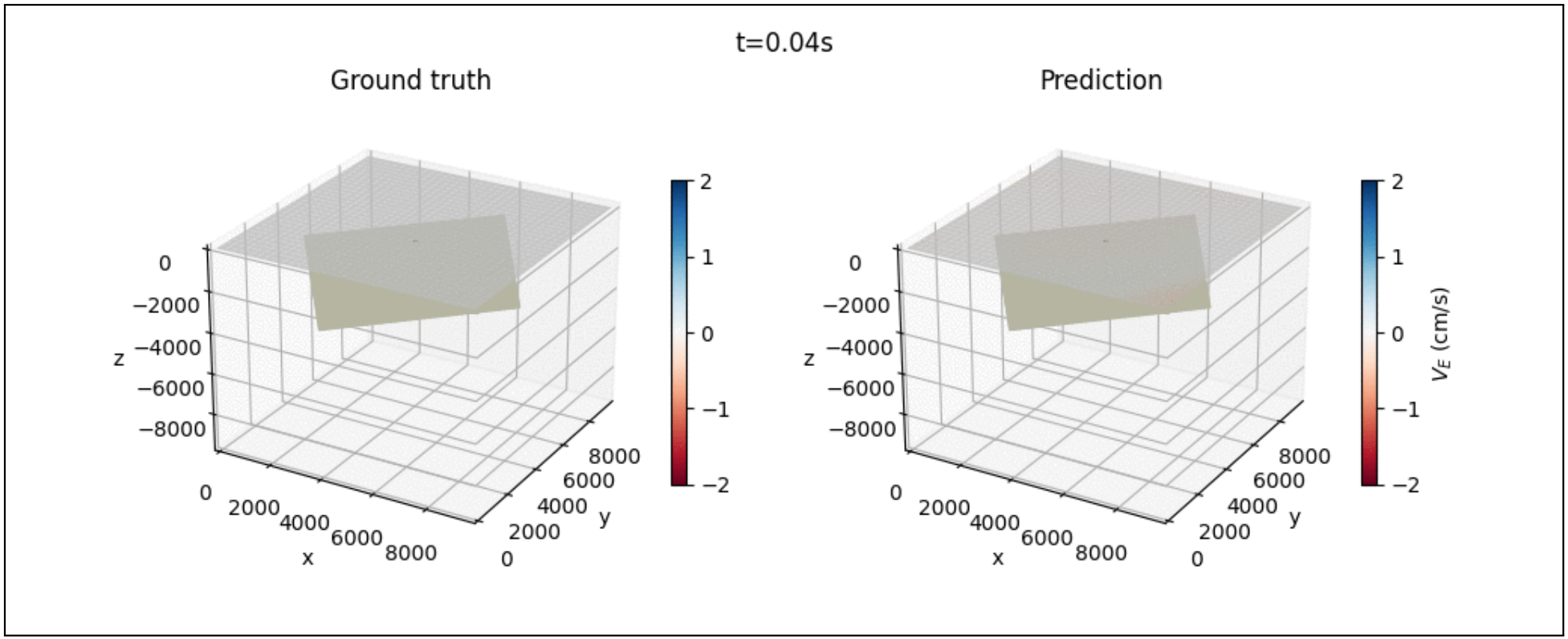


Figure – Source-to-site finite-fault simulation with MIFNO.

1. choose randomly one geology in the Le Teil database
2. for each point on the fault plane, predict the surface wavefields with the fine-tuned MIFNO
3. deconvolve all surface wavefields by the spice bench source time function
4. convolve each surface wavefield by the source time function corresponding to its associated point source
5. sum all surface wavefields

What’s next ?

Conclusions and perspectives

Summary Neural operators surrogate 3D elastodynamics :

- Learning Green's operator in heterogeneous media
- Learning Green's operator for any source position
- Extended faults via superposition
- Open-source database

Perspectives (ongoing)

- Including complex geometry (topography)
- Representation equivalence Bartolucci et al. [see 2]
- UQ for safety margin assessment

For further info: OMEIR Team webpage

Annexes

How to learn operators from discrete data in (separable) Hilbert spaces ?
$\{f_i\}_{i\in I} \subset \mathcal{H}$ is a *frame* iff :

$$\exists A, B > 0 \quad s.t. \quad A\|f\|^2 \leq \sum_{i\in I} |\langle f, f_i\rangle| \leq B\|f\|^2$$

- *Synthesis operator* : $T : \{c_i\}_{i\in I} \subset \ell^2(I) \mapsto \sum_{i\in I} c_i f_i \in \mathcal{H}$ (bounded $\|T\| \leq \sqrt{B}$)
- *Analysis operator* : $T^* : f \in \mathcal{H} \mapsto \{\langle f, f_i\rangle\}_{i\in I} \subset \ell^2(I)$ (bounded)
- *Frame operator* : $S = TT^*$ (bounded, positive, self-adjoint and invertible $\|S\|_{op} \leq B$)

$$Sf = \sum_{i\in I} \langle f, f_i\rangle f_i$$

- Pseudo-inverse : $T^\dagger : f \in \mathcal{H} \mapsto \left\{\left\langle f, S^{-1}f_i\right\rangle\right\}_{i\in I}$ ($\|T^\dagger\|_{op} \leq \frac{1}{\sqrt{A}}$)

$$f = TT^\dagger f = \sum_{i\in I} \left\langle f, S^{-1}f_i\right\rangle f_i = \sum_{i\in I} \langle f, f_i\rangle S^{-1}f_i$$

Countable $\{v_i\}_{i\in I} \subset \mathcal{H}$ is a frame sequence if frame for $\mathcal{V} := \overline{span}\,\{v_i : i \in I\} \subset \mathcal{H}$ (iff $T^* : \overline{span}\,\{v_i : i \in I\} \to \ell^2(I)$ injective, even if T^* not surjective$\to$ T not injective) :

$$P_{\mathcal{V}} f = \sum_{i\in I} \left\langle f, S^{-1} v_i \right\rangle v_i \qquad \varepsilon(f) = f - P_{\mathcal{V}} f$$

CDE : aliasing error $\|\varepsilon(f)\| = 0$!

$$\begin{array}{ccc} \mathcal{H} & \xrightarrow{\quad G \quad} & \mathcal{K} \\ \downarrow{\scriptstyle T_\Psi^\dagger} & & \uparrow{\scriptstyle T_\Phi} \\ \ell^2(I) & \xrightarrow{\quad g \quad} & \ell^2(K) \end{array}$$

Figure – Source : Bartolucci et al. [2]. $\mathcal{H} = L^2\left(\mathbb{R}^3\right)$, $\mathcal{K} = H_0^1(\mathbb{R}^+, H^1(\partial\Omega|_n)^3)$

$G : Dom(G) \subset \mathcal{H} \to \mathcal{K}$

$\mathcal{V}_\Phi = \overline{span}\,(\{\phi_i\}_{i\in I})$, $\mathcal{V}_\Psi = \overline{span}\left(\left\{\psi_j\right\}_{j\in J}\right)$: discrete operator $g : \ell^2(I) \to \ell^2(J)$

On the representation equivalence[2]
Operator aliasing

$$\varepsilon\left(G, g, \Psi, \Phi\right) = G - T_\Phi \circ g \circ T_\Psi^\dagger$$

Example

$f \in \mathcal{B}_\Omega := \left\{f \in L^2(\mathbb{R}) : supp(\hat{f}) \subset [-\Omega, \Omega]\right\}$ Whittaker-Shannon-Kotel'nikov sampling theorem : $f(x) = 2T\Omega \sum_{n\in\mathbb{Z}} f(nT) sinc(2\Omega(x - nT))$
$G : \mathcal{B}_\Omega \to \mathcal{B}_{2\Omega}$, $G : f \mapsto |f|^2$:

1. $\Psi = \Phi = \{sinc(2\Omega x - n)\}_{n\in\mathbb{Z}}$
   - Same grid $\left\{\frac{n}{2\Omega}\right\}_{n\in\mathbb{Z}}$
   - Discrete operator $g(\{c_n\}_{n\in\mathbb{Z}}) = T_\Psi^\dagger \circ G \circ T_\Psi(\{c_n\}_{n\in\mathbb{Z}}) = \left\{|c_n|^2\right\}_{n\in\mathbb{Z}}$
   - $\varepsilon\left(G, g, \Psi, \Phi\right)(f) = G(f) - \underbrace{T_\Phi T_\Psi^\dagger \circ G(f)}_{P_{\mathcal{B}_\Omega}(f)} \neq 0, \forall f \in \mathcal{B}_\Omega, G(f) \in \mathcal{B}_{2\Omega} \backslash \mathcal{B}_\Omega$
2. $\Psi = \{sinc(2\Omega x - n)\}_{n\in\mathbb{Z}}$, $\Phi = \{sinc(4\Omega x - n)\}_{n\in\mathbb{Z}}$
   - Double-resolution grid $\left\{\frac{n}{4\Omega}\right\}_{n\in\mathbb{Z}}$
   - $\mathcal{B}_\Omega \subset \mathcal{B}_{2\Omega}$
   - $\varepsilon\left(G, g, \Psi, \Phi\right)(f) = 0, \forall f \in \mathcal{B}_\Omega$ CDE !

On the representation equivalence[2]
Representation equivalence error

Discrete operator depends on the input/output frame sequences $\mathcal{V}_\Psi = \overline{span}\,(\Psi)$, $\mathcal{V}_\Phi = \overline{span}\,(\Phi)$

$$g(\Psi,\Phi) : RanT^\dagger_\Psi \to RanT^\dagger_\Phi$$

Note that : $T^\dagger_\Psi T_\Psi$ orthogonal projector onto $(Ker(T_\Psi))^\perp$ $RanT^\dagger_\Psi \subset \mathcal{H}$ (closed)
$\Longrightarrow f \in \mathcal{H}$ uniquely determined by $\{f_i\}_{i\in I} \subset RanT^\dagger_\Psi$

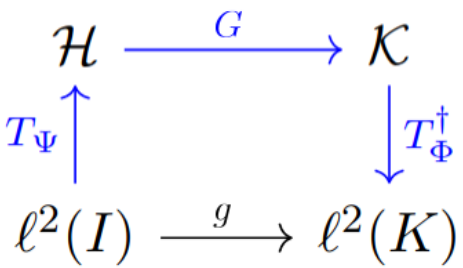
$$\tau\left(g,g'\right) = g - T^\dagger_\Phi \circ T_{\Phi'} \circ g' \circ T^\dagger_{\Psi'} \circ T_\Psi$$

Equivalent discrete representation : $\|\tau\left(g,g'\right)\| = 0$

Representation equivalent Neural Operators (ReNO) [2]

(G,g) are ReNO iff $\varepsilon(G,g,\Psi,\Phi) = 0$
Suff. condition : (Ψ,Φ) s.t. $Dom(G) \subset \mathcal{V}_\Psi$, $Ran(G) \subset \mathcal{V}_\Phi$

$$\Longrightarrow g\,(\Psi,\Phi) = T^\dagger_\Phi \circ G \circ T_\Psi : Ran(T^\dagger_\Psi) \to Ran(T_\Phi)$$



$$g(\Psi', \Phi') = T^{\dagger}_{\Phi'} \circ T_{\Phi} \circ g(\Psi, \Phi) \circ T^{\dagger}_{\Psi} \circ T_{\Psi'} \Longrightarrow \tau(\Psi, \Phi, \Psi', \Phi') = 0$$

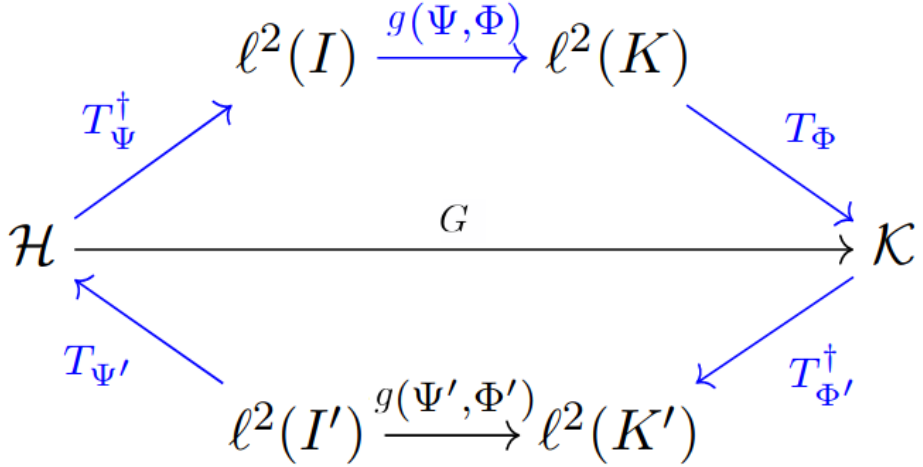


Figure – Representation equivalent Neural Operator (ReNO) [2]

On the representation equivalence[2]
Layer-wise instatiation

Multi-layer Neural Operator $G = H^{(\ell)} \circ \ldots \circ H^{(\ell)} \circ \ldots \circ H^{(0)}$, with with $H^{(\ell)} : \mathcal{H}_\ell \to \mathcal{H}_{\ell+1}$

- Unless $H^{(\ell)}$ is a ReNO $\forall \ell \in \{0, \ldots, L\} \Longrightarrow$ layer-wise aliasing error propagates
- It depends on the choice of $\Psi^{(\ell)}$
- Bartolucci et al. [2] : Aliasing may be kept small $\|\varepsilon(G, g, \Psi, \Phi)\| \leq \delta$: If (Ψ, Φ) and (Ψ', Φ') s.t. $Dom(G) \subset \mathcal{V}_\Psi \cap \mathcal{V}_{\Psi'}$, $Ran(G) \subset \mathcal{V}_\Phi \cap \mathcal{V}_{\Phi'}$ and $\mathcal{V}_{\Phi'} \subset \mathcal{V}_\Phi$

$$\|\tau(g, g')\| \leq \frac{2\delta\sqrt{B_\Psi}}{\sqrt{A_\Psi}}$$

F-FNO ?

$G_\theta = Q \circ H_F^{(\ell)} \circ H_F^{(\ell-1)} \circ \ldots H_F^{(0)} \circ P$?

Fourier layer $\boldsymbol{v}^{(\ell+1)} = H_F^{(\ell)} \boldsymbol{v}^{(\ell)}$:

$$\boldsymbol{v}^{(\ell+1)}\left(\boldsymbol{\xi}\right) = \sigma\left(\mathcal{F}^{-1}\left(\mathcal{R}^{(\ell)} \odot \mathcal{F}\left(\boldsymbol{v}^{(\ell)}\right)\left(\boldsymbol{\xi}\right)\right) + \boldsymbol{W}^{(\ell)}\boldsymbol{v}^{(\ell)}\left(\boldsymbol{\xi}\right) + \boldsymbol{b}^{(\ell)}\right) \tag{6}$$

To simplify ($\boldsymbol{W}^{(\ell)} = \boldsymbol{0}, \boldsymbol{b}^{(\ell)} = \boldsymbol{0}$) [8]

- Fourier layer : $G = \sigma\left(K^{(\ell)}\boldsymbol{v}^{(\ell)}\left(\boldsymbol{\xi}\right)\right) = \sigma\left(\mathcal{F}^{-1}\left(\mathcal{R}^{(\ell)} \odot \mathcal{F}\left(\boldsymbol{v}^{(\ell)}\right)\left(\boldsymbol{\xi}\right)\right)\right)$
  - $\mathcal{F} : w \in L^2\left(\mathbb{T}\right) \mapsto \left\{\left\langle w, ^{i\pi k\cdot}\right\rangle\right\}_{k\in\mathbb{Z}} \in \ell^2\left(\mathbb{Z}\right)$
  - $\mathcal{F}^{-1} : \{W_k\}_{k\in\mathbb{Z}} \in \ell^2\left(\mathbb{Z}\right) \mapsto \sum_{k\in\mathbb{Z}} W_k e^{i\pi kx}$
- Discretization (F, F^{-1} : DFT) :
  $g = \sigma\left(k^{(\ell)}\boldsymbol{v}^{(\ell)}\left(\boldsymbol{\xi}\right)\right) = \sigma\left(F^{-1}\left(R^{(\ell)} \odot F\left(\boldsymbol{v}^{(\ell)}\right)\left(\boldsymbol{\xi}\right)\right)\right)$
- CDE : $K > 0, \mathcal{P}_K := \left\{w(x) = \sum_{k=-K}^{K} W_K e^{i\pi kx}, \{W_k\}_{k=-K}^{K} \in \mathbb{C}^{2K+1}\right\} \subset \mathcal{B}_{\frac{K}{2}}$:

$$\mathcal{P}_K \ni w = \sum_{k=-K}^{K} w\left(\frac{k}{2K+1}\right)\Psi_k\left(\cdot\right), \quad \Psi_K = \left\{\frac{1}{\sqrt{2\left(2K+1\right)}} d\left(\cdot - \frac{2k}{2K+1}\right)\right\}_{k=0}^{2K}$$

d =Dirac's kernel and DFT coefficients $\hat{W}_k = (2K+1)W_k, k \in \{-K \ldots K\}$

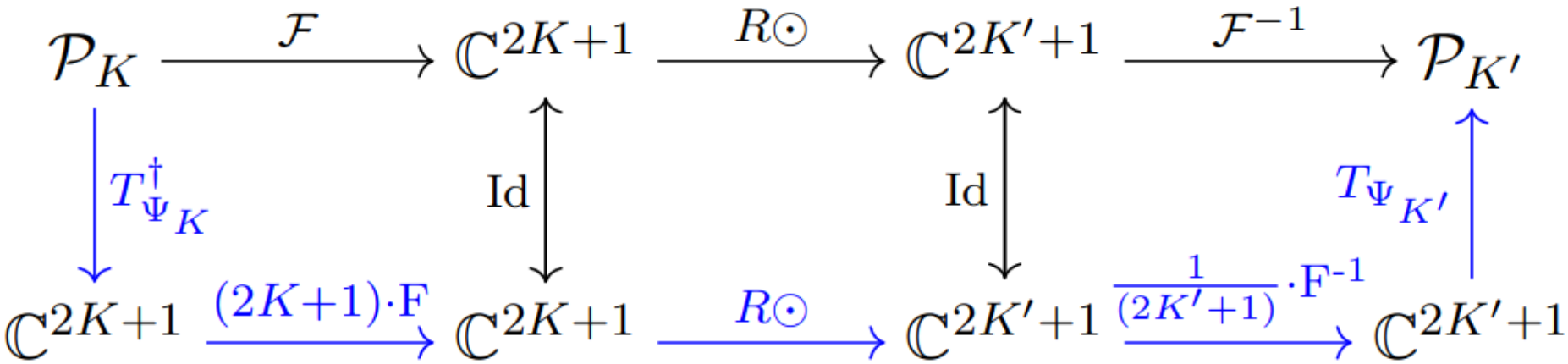


Figure – CDE for FNO. Reprinted from BARTOLUCCI et al. [2].

- $K^{'} \leq K$
- $R = \{R_k\}_{k-=-K'}^{K^{'}}$
- FNO (without activation) is a ReNO between bandlimited 2-periodic functions

$$(\mathcal{R} \odot \mathcal{F} w)(k) = R_k W_k, \quad k \in \left\{-K^{'}, \ldots, K^{'}\right\}$$

Activation function hampers CDE

$$\sigma(f) = ReLU(f) \notin \mathcal{P}_K$$

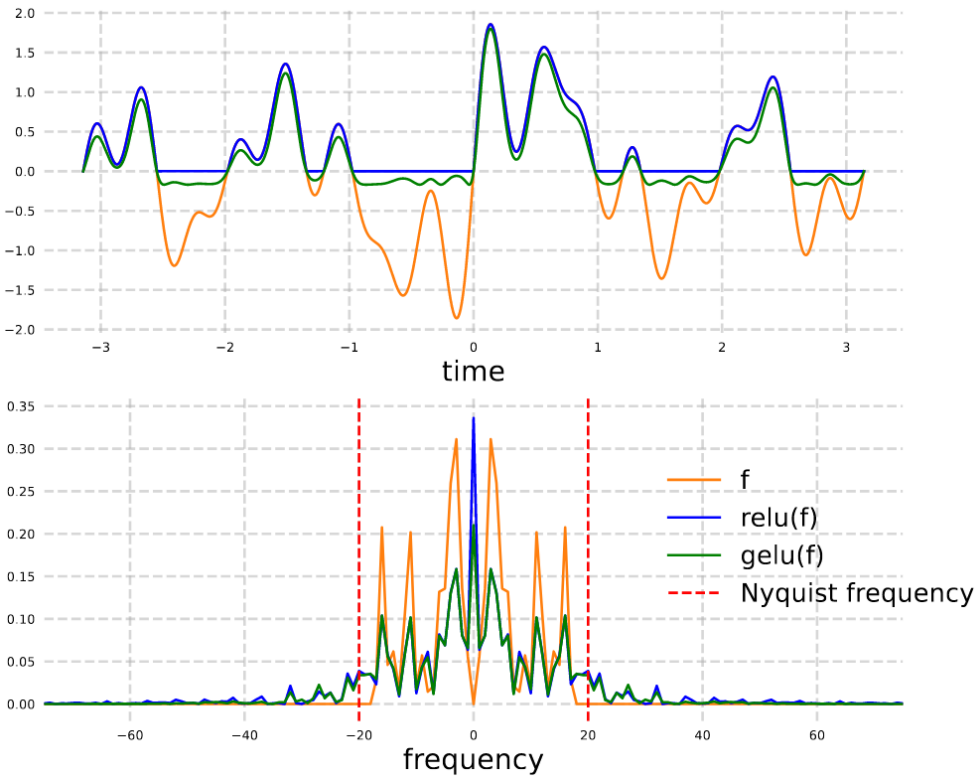


Figure – Activation function hampers CDE for FNO. Reprinted from Bartolucci et al. [2].

F-FNO Goodness of Fit metric

$$rMAE = \frac{1}{N_{val} N_x N_y} \sum_{n=1}^{N_{val}} \sum_{x,y} rMAE_n(x,y) \tag{7}$$

$$rRMSE = \frac{1}{N_{val} N_x N_y} \sum_{n=1}^{N_{val}} \sum_{x,y} rRMSE_n(x,y) \tag{8}$$

$$\mathrm{rFFT_{low}} = \frac{\overline{\mathcal{F}\left(\hat{V}(x,y)\right)}_{low} - \overline{\mathcal{F}\left(V(x,y)\right)}_{low}}{\overline{\mathcal{F}\left(V(x,y)\right)}_{low}} \tag{9}$$

with

$$\overline{\mathcal{F}\left(V(x,y)\right)}_{low} = \frac{1}{N_f} \sum_{0 \le f < 1} |\mathcal{F}(V(x,y))(f)| \tag{10}$$

Bibliography

Bibliography I

[1] **Aki, K. et Richards, P.G. *Quantitative Seismology-Theory and Methods*. Books in Geology. San Francisco (USA) : W.H Freeman et Company, 1980.**

[2] **Bartolucci, Francesca et al. "Representation Equivalent Neural Operators : a Framework for Alias-free Operator Learning". en. In : arXiv :2305.19913 (nov. 2023). arXiv :2305.19913 [cs, eess]. URL : http://arxiv.org/abs/2305.19913.**

[3] **Carvalho Paludo, L. de, Bouvier, V. et Cottereau, R. "Scalable parallel scheme for sampling of Gaussian random fields over very large domains".** In : *International Journal for Numerical Methods in Engineering* 117.8 (2019). doi : 10.1002/nme.5981, p. 845-859. DOI : 10.1002/nme.5981. eprint : https://onlinelibrary.wiley.com/doi/pdf/10.1002/nme.5981. URL : https://onlinelibrary.wiley.com/doi/abs/10.1002/nme.5981.

[4] **CEA and CentraleSupélec and IPGP and CNRS. "SEM3D Ver 2017.04 Registered at French Agency for Protection of Programs (Dépôt APP)".** IDDN.FR.001.400009.000.S.P.2018.000.31235. 2017.

Bibliography III

[5] **Gatti, F. et al. "3-D source-to-site numerical investigation on the earthquake ground motion coherency in heterogeneous soil deposits".** In : *9th European Conference on Numerical Methods in Geotechnical Engineering, 25-27 June 2018, Porto (Portugal)*. 2018.

[6] **Korres, M. et al. "Enhanced Seismic Response Prediction of Critical Structures via 3D Regional Scale Physics-Based Earthquake Simulation".** en. In : *Journal of Earthquake Engineering* (jan. 2022), p. 1-29. ISSN : 1363-2469, 1559-808X. DOI : 10.1080/13632469.2021.2009061. URL : https://www.tandfonline.com/doi/full/10.1080/13632469.2021.2009061.

Bibliography IV

[7] **Lehmann, Fanny et al. "3D elastic wave propagation with a Factorized Fourier Neural Operator (F-FNO)".** en. In : *Computer Methods in Applied Mechanics and Engineering* 420 (fév. 2024), p. 116718. ISSN : 00457825. DOI : 10.1016/j.cma.2023.116718. URL : https://linkinghub.elsevier.com/retrieve/pii/S0045782523008411.

[8] **Li, Zongyi et al. "Fourier Neural Operator for Parametric Partial Differential Equations".** en. In : arXiv :2010.08895 (mai 2021). arXiv :2010.08895 [cs, math]. URL : http://arxiv.org/abs/2010.08895.

[9] **Molinari, Irene et Morelli, Andrea. "EPcrust : A reference crustal model for the European plate".** In : *Geophys. J. Int.* 185.1 (2011), p. 352-364. DOI : 10.1111/j.1365-246X.2011.04940.x.

[10] **Touhami, S. et al. "SEM3D : A 3D high-fidelity numerical earthquake simulator for broadband (0-10 hz) seismic response prediction at a regional scale".** In : *Geosciences* 12.3 (2022). DOI : 10.3390/geosciences12030112. URL : https://www.mdpi.com/2076-3263/12/3/112.

[11] **Tran, Alasdair et al. "Factorized Fourier Neural Operators".** In : arXiv :2111.13802 (mars 2023). arXiv :2111.13802 [cs]. URL : http://arxiv.org/abs/2111.13802.